Table 1
Results of site-specific glycosylation analysis of human CP

Retention time (min)	Glycopeptides		Calculated MW	Relative peak intensity[a] (%)	Peptide		Oligosaccharide		
	m/z	Charge			Sequence	Theoretical MW	Calculated MW	Theoretical MW	Composition[b,c]
26	1415.3	+3	4242.8	52	EHEGAIYPDN[119]TTDFQR	1891.8	2369.0	2368.8	[HexNAc]4[Hex]5[NeuAc]2[Fuc]1
26	1366.6	+3	4096.7	100	EHEGAIYPDN[119]TTDFQR	1891.8	2223.0	2222.8	[HexNAc]4[Hex]5[NeuAc]2
27	1682.7	+3	5045.1	6	EHEGAIYPDN[119]TTDFQR	1891.8	3171.3	3171.1	[HexNAc]5[Hex]6[NeuAc]3[Fuc]2
27	1634.0	+3	4899.0	21	EHEGAIYPDN[119]TTDFQR	1891.8	3025.2	3025.1	[HexNAc]5[Hex]6[NeuAc]3[Fuc]1
27	1225.8	+4	4899.0						
27	1585.3	+3	4753.0	24	EHEGAIYPDN[119]TTDFQR	1891.8	2879.2	2879.0	[HexNAc]5[Hex]6[NeuAc]3
27	1189.3	+4	4753.0						
28	1458.3	+3	4372.0	35	ELHHLQEQN[743]VSNAFLDK	2021.0	2369.0	2368.8	[HexNAc]4[Hex]5[NeuAc]2[Fuc]1
28	1409.6	+3	4225.9	100	ELHHLQEQN[743]VSNAFLDK	2021.0	2222.9	2222.8	[HexNAc]4[Hex]5[NeuAc]2
28	1057.5	+4	4225.9						
29	1725.8	+3	5174.5	5	ELHHLQEQN[743]VSNAFLDK	2021.0	3171.5	3171.1	[HexNAc]5[Hex]6[NeuAc]3[Fuc]2
29	1294.6	+4	5174.2						
29	1677.1	+3	5028.2	29	ELHHLQEQN[743]VSNAFLDK	2021.0	3025.3	3025.1	[HexNAc]5[Hex]6[NeuAc]3[Fuc]1
29	1258.1	+4	5028.2						
29	1628.4	+3	4882.1	43	ELHHLQEQN[743]VSNAFLDK	2021.0	2879.1	2879.0	[HexNAc]5[Hex]6[NeuAc]3
29	1221.5	+4	4882.1						
31[d]	1895.8	+3	5684.4	2	ELHHLQEQN[743]VSNAFLDK	2021.0	3681.4	3681.3	[HexNAc]6[Hex]7[NeuAc]4[Fuc]1
31[d]	1422.1	+4	5684.3						
31[d]	1847.1	+3	5538.4	3	ELHHLQEQN[743]VSNAFLDK	2021.0	3535.4	3535.2	[HexNAc]6[Hex]7[NeuAc]4
31	1385.6	+4	5538.3						
35[d]	1493.3	+3	4477.0	6	EN[378]LTAPGSDSAVFFEQGTTR	2126.0	2369.0	2368.8	[HexNAc]4[Hex]5[NeuAc]2[Fuc]1
35	1444.6	+3	4330.9	100	EN[378]LTAPGSDSAVFFEQGTTR	2126.0	2222.9	2222.8	[HexNAc]4[Hex]5[NeuAc]2
37	1712.1	+3	5133.2	8	EN[378]LTAPGSDSAVFFEQGTTR	2126.0	3025.2	3025.1	[HexNAc]5[Hex]6[NeuAc]3[Fuc]1
37	1284.3	+4	5133.2						
37	1663.4	+3	4987.1	23	EN[378]LTAPGSDSAVFFEQGTTR	2126.0	2879.2	2879.0	[HexNAc]5[Hex]6[NeuAc]3
37	1247.8	+4	4987.2						
39	1331.3	+3	3990.8	14	AGLQAFFQVQECN[339]K	1639.7	2369.1	2368.8	[HexNAc]4[Hex]5[NeuAc]2[Fuc]1
39	1923.4	+2	3844.7		AGLQAFFQVQECN[339]K	1639.7	2223.0	2222.8	[HexNAc]4[Hex]5[NeuAc]2
39	1282.6	+3	3844.7	100					
41	1501.3	+3	4500.8	6	AGLQAFFQVQECN[339]K	1639.7	2879.2	2879.0	[HexNAc]5[Hex]6[NeuAc]3

Note. All masses are monoisotopic. Cysteine residue was carboxymethylated.

[a] Relative peak intensity was calculated by comparing same charge state glycopeptide ions. The intensity of the glycoform with maximum at each glycosylation site was taken as 100%.

[b] The oligosaccharide composition was deduced from the molecular weight of the oligosaccharide.

[c] The glycopeptide ions adducted by NH_4^+ or Na^+ were excluded.

[d] Product ion spectra of these molecular ions were not acquired. However, these were considered glycopeptides because of a molecular weight difference of 146 (Fuc) and the same retention time as other glycopeptides.

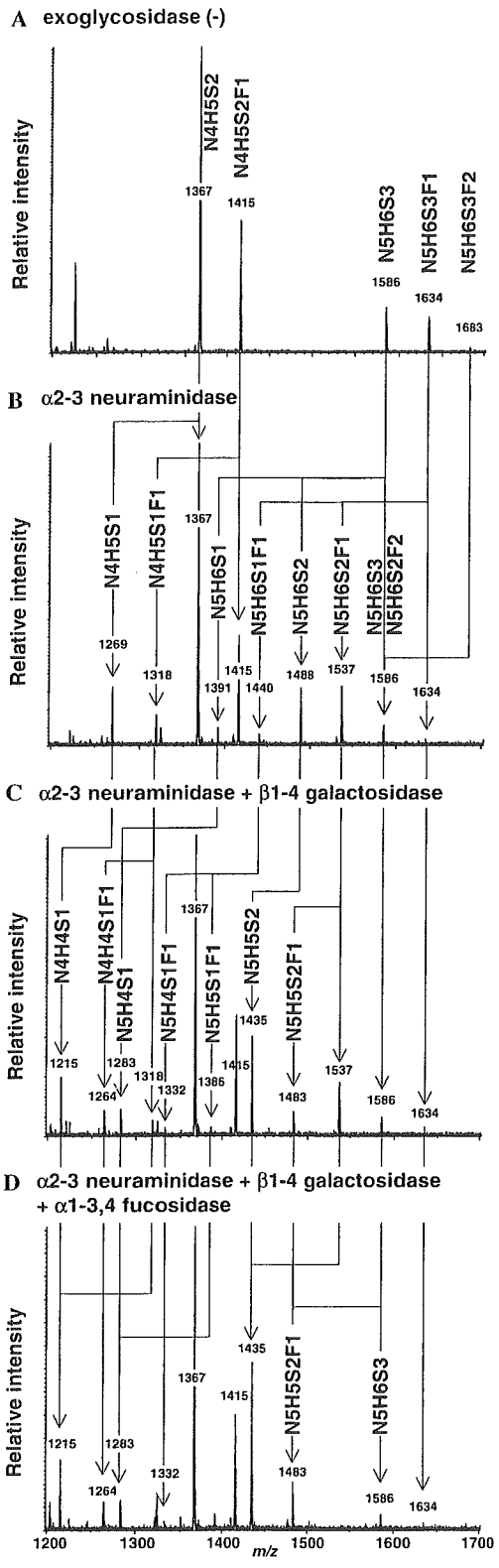

Fig. 5. LC-ESI mass spectra of the glycopeptides containing Asn119 digested with the following exoglycosidases: (A) exoglycosidase (−); (B) α2–3 neuraminidase; (C) α2–3 neuraminidase + β1–4 galactosidase; (D) α2–3 neuraminidase + β1–4 galactosidase + α1–3,4 fucosidase. Arrows between panels A and B, panels B and C, and panels C and D correspond to the digestion of NeuAc, Gal, and Gal+Fuc, respectively. H, hexose; N, *N*-acetylhexosamine; F, fucose; S, *N*-acetylneuraminic acid.

of Asn378 glycopeptides showed lower core fucosylation, and that of Asn339 glycopeptides showed lower branching. These glycosylation profiles provided the heterogeneity of fucose linkage and the number of arms at each glycosylationsite in human CP.

Discussion

A site-specific glycosylation analysis of human CP was conducted using LC-ESI-MS/MS, where product ion spectra were acquired in a data-dependent manner. The collision energy for the product ion scan was adjusted from 30 to 80 eV depending on the size and charge of the precursor ion. Under these conditions, peptide precursor ions were degraded and produced b- and y-series fragment ions derived from the amino acid sequence. Glycopeptide precursor ions produced abundant carbohydrate ions (*m/z* 204, 186, 168, and 366) together with several low intensity b- and y-series fragment ions derived from the amino acid sequence [20,21]. Thus, product ion spectra of glycopeptides are readily distinguishable from those of peptides by such carbohydrate marker ions, and the peptide moiety in the glycopeptide could be deduced from the product ions that were consistent with the expected fragment ions derived from the peptide containing the N-glycosylation site. It is known that the glycopeptide ions are more labile than peptide ions and produce consecutive monosaccharide/polysaccharide losses at much lower collision energy, and this would provide information about branching and fucose location [18]. However, we used relatively high collision energy in this site-specific glycosylation analysis to identify the peptide ions in parallel with the detection and identification of the glycopeptide ions.

Protein coverage of more than 70% in human CP was obtained in the LC-ESI-MS/MS analysis with the *m/z* range of 400–2000 (for peptide mapping). The heterogeneity at four potential N-glycosylation sites was determined in the *m/z* range of 1000–2000 (glycosylation analysis). We could detect all of the potential glycosylation sites as either glycopeptides or nonglycosylated peptides. Peptides containing the potential N-glycosylation site Asn208, Asn569, or Asn907 were detected in nonglycosylated but not glycosylated forms. Peptides with the potential N-glycosylation site Asn119, Asn339, Asn378 or Asn743 were detected in glycosylated but not nonglycosylated forms. These findings indicate that Asn119, Asn339, Asn378, and Asn743 of human CP are glycosylated and that Asn208, Asn569, and Asn907 are not. Human CP was reported to have no O-linked glycosylation [8]. No information on O-glycosylation was obtained from this analysis. These results are consistent with a previous study determining the glycosylation sites of human CP [9].

Heterogeneity of oligosaccharides was determined at each of four glycosylation sites. Disialobiantennary structures with no fucose or one fucose ($[HexNAc]_4$ $[Hex]_5$ $[NeuAc]_2[Fuc]_{0-1}$) and trisialotriantennary structures

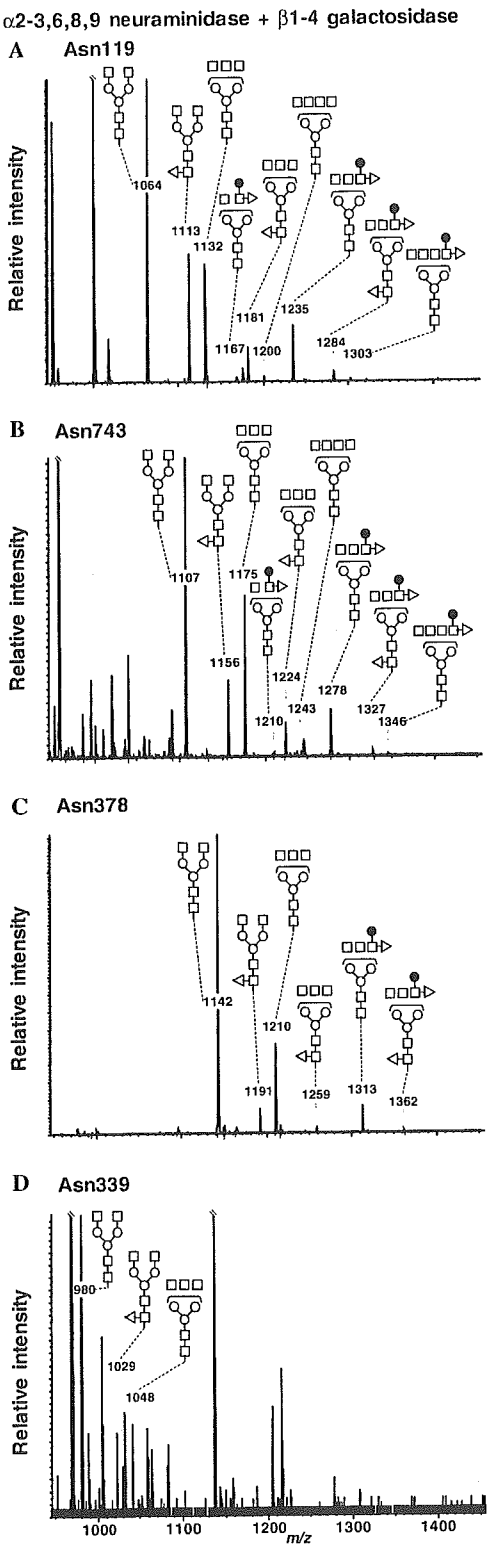

Fig. 6. LC-ESI mass spectra of the glycopeptides containing Asn119 (A), Asn743 (B), Asn378 (C), and Asn339 (D) after digestion with α2–3,6,8,9 neuraminidase + β1–4 galactosidase. Glycosylation profiles showed different degrees of branching and fucosylation at core GlcNAc and outer arm GlcNAc between glycosylation sites. Open circles, mannose; closed circles, galactose; open squares, *N*-acetyl glucosamine; open triangles, fucose.

($[HexNAc]_5[Hex]_6[NeuAc]_3$) were observed at all sites. These dominant oligosaccharides were consistent with structures published previously [7,8]. Furthermore, we detected trisialotriantennary structures with one fucose ($[HexNAc]_5[Hex]_6[NeuAc]_3[Fuc]_1$) at Asn119, Asn378, and Asn743, trisialotriantennary structures with two fucoses ($[HexNAc]_5[Hex]_6[NeuAc]_3[Fuc]_2$) at Asn119 and Asn743, and tetrasialotetraantennary structures with no fucose or one fucose ($[HexNAc]_6[Hex]_7[NeuAc]_4[Fuc]_{0-1}$) at Asn743.

To determine the linkage of fucose and NeuAc, exoglycosidase digestions were performed. Treatment with α2–3 neuraminidase suggested that roughly one antenna of triantennary glycans was linked by NeuAc in the α2–3 position. This is consistent with the previous findings that NeuAc is linked α2–3 to the Galβ1–4GlcNAcβ1–4Manα1–3Manβ1–4GlcNAcβ1–4GlcNAc group in the triantennary glycan in human CP [7,8]. Results from α2–3 neuraminidase + β1–4 galactosidase treatments with or without α1–3,4 fucosidase suggested that fucose residues were linked to reducing end GlcNAc and/or outer arm GlcNAc in the α1–3 position in the antenna where NeuAc is linked to galactose in the α2–3 position. These findings indicated that human CP contains a certain amount of sialyl Lewis X structure in triantennary glycans. Treatment with α2–3,6,8,9 neuraminidase + β1–4 galactosidase reveals the heterogeneity of the location of fucosylation as well as the number of arms. Although relative peak intensity does not express the relative amount of each glycan due to the different ionization efficiencies, the mass spectra showed the difference in fucosylation pattern and number of arms among sites.

No asialo oligosaccharides were detected in this analysis. It is known that desialylated CP is rapidly cleared from the circulation by the asialoglycoprotein receptor within the parenchymal cells of liver [27,28]. It is possible that desialylated CP might be cleared immediately by the liver.

Although the N-linked carbohydrate structures linked to human CP have been studied, only a few carbohydrate structures have been reported and site-specific characterization of these oligosaccharides has not been described. To determine the glycosylation state at each glycosylation site, the tryptic digest was examined by LC-ESI-MS/MS, where product ion spectra were acquired data-dependently. Glycopeptide ions were assigned based on the product ion spectra. Fucose and NeuAc linkages were determined by exoglycosidase digestions. Our data successfully provided comprehensive information on the site-specific N-linked oligosaccharides in human CP. This method is a powerful technique for elucidating the glycosylation of a biological sample.

Acknowledgments

This study was supported by a Grant-in-Aid for Research on Health Sciences focusing on Drug Innovation from the Japan Health Sciences Foundation.

References

[1] S. Osaki, D.A. Johnson, E. Frieden, The possible significance of the ferrous oxidase activity of ceruloplasmin in normal human serum, J. Biol. Chem. 241 (1966) 2746–2751.

[2] K. Yoshida, K. Furihata, S. Takeda, A. Nakamura, K. Yamamoto, H. Morita, S. Hiyamuta, S. Ikeda, N. Shimizu, N. Yanagisawa, A mutation in the ceruloplasmin gene is associated with systemic hemosiderosis in humans, Nat. Genet. 9 (1995) 267–272.

[3] Z.L. Harris, Y. Takahashi, H. Miyajima, M. Serizawa, R.T. MacGillivray, J.D. Gitlin, Aceruloplasminemia: molecular characterization of this disorder of iron metabolism, Proc. Natl. Acad. Sci. USA 92 (1995) 2539–2543.

[4] Z.L. Harris, A.P. Durley, T.K. Man, J.D. Gitlin, Targeted gene disruption reveals an essential role for ceruloplasmin in cellular iron efflux, Proc. Natl. Acad. Sci. USA 96 (1996) 10812–10817.

[5] N. Takahashi, T.L. Ortel, F.W. Putnam, Single-chain structure of human ceruloplasmin: the complete amino acid sequence of the whole molecule, Proc. Natl. Acad. Sci. USA 81 (1984) 390–394.

[6] M.L. Koschinsky, W.D. Funk, B.A. van Oost, R.T. MacGillivray, Complete cDNA sequence of human preceruloplasmin, Proc. Natl. Acad. Sci. USA 83 (1986) 5086–5090.

[7] K. Yamashita, C.J. Liang, S. Funakoshi, A. Kobata, Structural studies of asparagine-linked sugar chains of human ceruloplasmin. Structural characteristics of the triantennary complex type sugar chains of human plasma glycoproteins, J. Biol. Chem. 256 (1981) 1283–1289.

[8] M. Endo, K. Suzuki, K. Schmid, B. Fournet, Y. Karamanos, J. Montreuil, L. Dorland, H. van Halbeek, J.F. Vliegenthart, The structures and microheterogeneity of the carbohydrate chains of human plasma ceruloplasmin: a study employing 500-MHz ^{1}H-NMR spectroscopy, J. Biol. Chem. 257 (1982) 8755–8760.

[9] N. Takahashi, Y. Takahashi, T.L. Ortel, J.N. Lozier, N. Ishioka, F.W. Putnam, Purification of glycopeptides of human plasma proteins by high-performance liquid chromatography, J. Chromatogr. 317 (1984) 11–26.

[10] R.J. Cousins, Absorption, transport, and hepatic metabolism of copper and zinc: special reference to metallothionein and ceruloplasmin, Physiol. Rev. 65 (1985) 238–309.

[11] A. Mackiewicz, M.K. Ganapathi, D. Schultz, I. Kushner, Monokines regulate glycosylation of acute-phase proteins, J. Exp. Med. 166 (1987) 253–258.

[12] J.E. Hansen, J. Iversen, A. Lihme, T.C. Bog-Hansen, Acute phase reaction, heterogeneity, and microheterogeneity of serum proteins as nonspecific tumor markers in lung cancer, Cancer 60 (1987) 1630–1635.

[13] A. Senra Varela, J.J. Lopez Saez, D. Quintela Senra, Serum ceruloplasmin as a diagnostic marker of cancer, Cancer Lett. 121 (1997) 139–145.

[14] V. Ling, A.W. Guzzetta, E. Canova-Davis, J.T. Stults, W.S. Hancock, T.R. Covey, B.I. Shushan, Characterization of the tryptic map of recombinant DNA derived tissue plasminogen activator by high-performance liquid chromatography-electrospray ionization mass spectrometry, Anal. Chem. 63 (1991) 2909–2915.

[15] S.A. Carr, M.J. Huddleston, M.F. Bean, Selective identification and differentiation of N- and O-linked oligosaccharides in glycoproteins by liquid chromatography–mass spectrometry, Protein Sci. 2 (1993) 183–196.

[16] M.J. Huddleston, M.F. Bean, S.A. Carr, Collisional fragmentation of glycopeptides by electrospray ionization LC/MS and LC/MS/MS: methods for selective detection of glycopeptides in protein digests, Anal. Chem. 65 (1993) 877–884.

[17] P.A. Schindler, C.A. Settineri, X. Collet, C.J. Fielding, A.L. Burlingame, Site-specific detection and structural characterization of the glycosylation of human plasma proteins lecithin:cholesterol acyltransferase and apolipoprotein D using HPLC/electrospray mass spectrometry and sequential glycosidase digestion, Protein Sci. 4 (1995) 791–803.

[18] M.A. Ritchie, A.C. Gill, M.J. Deery, K. Lilley, Precursor ion scanning for detection and structural characterization of heterogeneous glycopeptide mixtures, J. Am. Soc. Mass Spectrom. 13 (2002) 1065–1077.

[19] F. Wang, A. Nakouzi, R.H. Angeletti, A. Casadevall, Site-specific characterization of the N-linked oligosaccharides of a murine immunoglobulin M by high-performance liquid chromatography/electrospray mass spectrometry, Anal. Biochem. 314 (2003) 266–280.

[20] J.F. Nemeth, G.P. Hochgesang Jr., L.J. Marnett, R.M. Caprioli, Characterization of the glycosylation sites in cyclooxygenase-2 using mass spectrometry, Biochemistry 40 (2001) 3109–3116.

[21] O. Krokhin, W. Ens, K.G. Standing, J. Wilkins, H. Perreault, Site-specific N-glycosylation analysis: matrix-assisted laser desorption/ionization quadrupole–quadrupole time-of-flight tandem mass spectral signatures for recognition and identification of glycopeptides, Rapid Commun. Mass Spectrom. 18 (2004) 2020–2030.

[22] A. Harazono, N. Kawasaki, T. Kawanishi, T. Hayakawa, Site-specific glycosylation analysis of human apolipoprotein B100 using LC/ESI MS/MS, Glycobiology 15 (2005) 447–462.

[23] C.W. Sutton, J.A. O'Neill, J.S. Cottrell, Site-specific characterization of glycoprotein carbohydrates by exoglycosidase digestion and laser desorption mass spectrometry, Anal. Biochem. 218 (1994) 34–46.

[24] P. Roepstorff, J. Fohlman, Proposal for a common nomenclature for sequence ions in mass spectra of peptides, Biomed. Mass Spectrom. 11 (1984) 601.

[25] K. Maemura, M. Fukuda, Poly-*N*-acetyllactosaminyl *O*-glycans attached to leukosialin: the presence of sialyl Le(x) structures in *O*-glycans, J. Biol. Chem. 267 (1992) 24379–24386.

[26] S. Hemmerich, S.D. Rosen, 6'-Sulfated sialyl Lewis X is a major capping group of GlyCAM-1, Biochemistry 33 (1994) 4830–4835.

[27] C.J. Van Den Hamer, A.G. Morell, I.H. Scheinberg, J. Hickman, G. Ashwell, Physical and chemical studies on ceruloplasmin: IX. The role of galactosyl residues in the clearance of ceruloplasmin from the circulation, J. Biol. Chem. 245 (1970) 4397–4402.

[28] A.G. Morell, G. Gregoriadis, I.H. Scheinberg, J. Hickman, G. Ashwell, The role of sialic acid in determining the survival of glycoproteins in the circulation, J. Biol. Chem. 246 (1971) 1461–1467.

RAPID COMMUNICATIONS IN MASS SPECTROMETRY
Rapid Commun. Mass Spectrom. 2005; **19**: 3315–3321
Published online 31 October 2005 in Wiley InterScience (www.interscience.wiley.com). DOI: 10.1002/rcm.2190

Specific detection of Lewis x-carbohydrates in biological samples using liquid chromatography/multiple-stage tandem mass spectrometry

Noritaka Hashii[1,2], Nana Kawasaki[1,2]*, Satsuki Itoh[1], Akira Harazono[1], Yukari Matsuishi[1,2], Takao Hayakawa[3] and Toru Kawanishi[1]

[1]Division of Biological Chemistry and Biologicals, National Institute of Health Sciences, 1-18-1 Kamiyoga, Setagaya-ku, Tokyo 158-8501, Japan
[2]Core Research for Evolutional Science and Technology (CREST) of Japan Science and Technology Agency (JST), Kawaguchi Center Building, 4-1-8 Hon-cho, Kawaguchi, Saitama 332-0012, Japan
[3]Pharmaceutical and Medical Devices Agency, 3-3-2 Kasumigaseki, Chiyoda-ku, Tokyo 100-0013, Japan

Received 14 July 2005; Revised 5 September 2005; Accepted 8 September 2005

The Lewis x structure [Le^x, Galβ1-4(Fucα1-3)GlcNAc] motif is one of the tumor antigens and plays an important role in oncogenesis, development, cellular differentiation and adhesion. The detection of Le^x-carbohydrates and their structural analysis are necessary to clarify the role of Le^x in several biological events. Mass spectrometry has been preferably used for the structural analysis of carbohydrates. Especially, collision-induced dissociation (CID) tandem mass spectrometry (MS/MS), which causes a glycosidic bond cleavage, is used for carbohydrate sequencing. However, Le^x cannot be identified by MS/MS due to the existence of the positional isomers, such as Lewis a [Galβ1-3(α1-4Fuc)GlcNAc]. In the present study, we demonstrate the specific detection of Le^x-carbohydrates in a biological sample by using multiple-stage MS/MS (MS^n). Using pyridylaminated oligosaccharides bearing Le^x, we found that the Le^x-motif yields a cross-ring fragment by the cleavage of a bond between C-3 and C-4 of GlcNAc in Gal(Fuc)GlcNAc. The Le^x-specific cross-ring fragment ion at *m/z* 259 was effectively detected by sequential scans, consisting of a full MS^1 scan, data-dependent CID MS^2 scan, MS^3 of [Gal(Fuc)GlcNAc+Na]$^+$ at *m/z* 534, and MS^4 of [GalGlcNAc+Na]$^+$ at *m/z* 388. The sequential scan was applied to *N*-linked oligosaccharide profiling using a LC/ESI-MS^n system equipped with a graphitized carbon column. We successfully detected the Le^x-motif and elucidated the structures of several Le^x and Lewis y [(Fucα1-2)Galβ1-4(Fucα1-3)GlcNAc] oligosaccharides in the murine kidney used as a model tissue. Our method is expected to be a powerful tool for the specific detection of the Le^x-motif, and structural elucidation of Le^x-carbohydrates in biological samples. Copyright © 2005 John Wiley & Sons, Ltd.

The Lewis x structure [Le^x, Galβ1-4(Fucα1-3)GlcNAc] is one of the tumor antigens, and plays an important role in oncogenesis[1,2] (abbreviations used here are: Gal, galactose; Fuc, fucose; GlcNAc, *N*-acetylglucosamine). Particularly, sialylated Le^x is used as a marker of lung, pancreas and uterus tumors.[3] Le^x and its derivatives are also known to be oligosaccharide ligands of some endothelial receptors, such as the selectins and the scavenger receptor, C-type lectin,[4,5] and affect embryonic development, cellular differentiation and adhesion.[6,7] However, the structural details of the oligosaccharides attached to the Le^x structure (Le^x-oligosaccharide) are still unclear. Le^x structure-specific detection and elucidation methods are necessary for the diagnosis of tumors and a study on the role of Le^x on various biological events.

Mass spectrometry (MS) has become very popular for the structural analysis of oligosaccharides. Low-energy collision-induced dissociation (CID) tandem mass spectrometry (MS/MS), which generates B/Y-series ions by glycosidic bond cleavage, is preferably used for oligosaccharide sequencing.[8–13] However, the detection of Le^x by MS/MS is still challenging due to the presence of its positional isomer, Lewis a [Le^a, Galβ1-3(Fucα1-4)GlcNAc]. The structural difference between Le^x and Le^a is the linkage at positions 3 or 4 of the non-reducing terminal fucose and galactose to GlcNAc (Fig. 1). For the linkage analysis, multiple-stage MS/MS (MS^n) pattern-matching, in which the oligosaccharide structure can be deduced from intensity ratios of fragment ions generated by MS^n, has recently been reported;[14–16] however, this method needs an identical analytical condition and various oligosaccharide standards. As an alternative method, the cross-ring fragmentation caused by MS^n is

Correspondence to: N. Kawasaki, Division of Biological Chemistry and Biologicals, National Institute of Health Sciences, 1-18-1 Kamiyoga, Setagaya-ku, Tokyo 158-8501, Japan.
E-mail: nana@nihs.go.jp
Contract/grant sponsor: Ministry of Health Labor and Welfare, and Core Research for the Evolutional Science and Technology Program, Japan Science and Technology Corp.

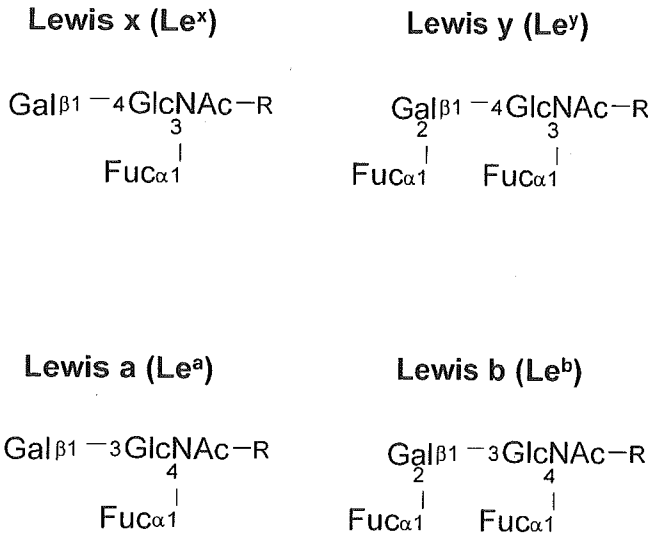

Figure 1. Structures of Lewis a, b, x and y.

sometimes used.[10,17,18] Meisen *et al.*[19] demonstrated that α2-6-linked *N*-acetylneuraminic acid (NeuNAc) can be distinguished from α2-3-linked NeuNAc based on structure-specific cross-ring fragment ions generated by low-energy CID MS^2 in the negative ion mode. Le^x could be expected to be distinguished from its positional isomers by cross-ring fragmentation.

In this study, we demonstrate the specific detection of Le^x-carbohydrates in a biological sample by using MS^n. Using pyridylaminated oligosaccharides bearing Le^x, we found that the Le^x-motif yields a cross-ring fragment by the cleavage of a bond between C-3 and C-4 of GlcNAc in Gal(Fuc)GlcNAc. The Le^x-specific cross-ring fragment ion at *m/z* 259 was effectively detected by sequential scans, consisting of a full MS^1 scan, data-dependent CID MS^2 scan, MS^3 of $[Gal(Fuc)GlcNAc+Na]^+$ at *m/z* 534, and MS^4 of $[GalGlcNAc+Na]^+$ at *m/z* 388 using nano-electrospray ionization-ion trap mass spectrometry (nanoESI-ITMS) in positive ion mode. Then, sequential MS^{1-4} scanning for the Le^x-characteristic ions was applied for *N*-linked oligosaccharide profiling using an LC/ESI-ITMS instrument equipped with a graphitized carbon column (GCC), by which diverse oligosaccharides, including isomers, can be separated. We successfully detected the Le^x-motif and subsequently elucidated the entire structure of Le^x-oligosaccharides in the model tissue, murine kidney, in which Le^x-oligosaccharides are abundantly present.[20]

EXPERIMENTAL

Materials

2-Aminopyridine (PA)-labeled pentasaccharides bearing Le^x (oligosaccharide I, Fig. 2(A)) or Le^a (oligosaccharide II, Fig. 2(B)), and the asialotriantennary oligosaccharide bearing Le^x (oligosaccharide III, Fig. 2(C)), were purchased from Takara Biomedicals (Otsu, Japan). Murine kidneys (MRL/MpJ-+/+) were purchased from Japan SLC Inc. (Hamamatsu, Japan).

Sample preparation

Proteins from murine kidneys were solubilized in lysis buffer (7 M urea, 2 M thiourea, 2% CHAPS, 30 mM Tris-HCl) by vortexing at room temperature. The proteins (100 μg) were recovered by precipitation in cold acetone, and then treated with 10 units of PNGase F in 500 μL of 0.2 M phosphate buffer (pH 7.6) at 37°C for 48 h to release the *N*-linked oligosaccharides. Proteins were removed by precipitation in cold ethanol, and the supernatant containing oligosaccharides was evaporated and lyophilized. The dried oligosaccharides were labeled with PA according to a previous report.[21] The PA-labeled oligosaccharides were desalted with Envi-Carb C (Supelco Bellefonte, USA) and lyophilized.

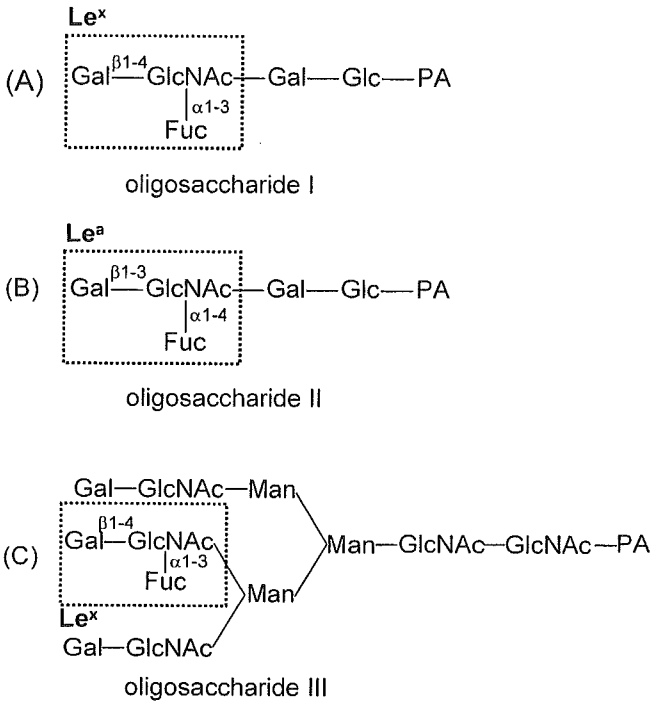

Figure 2. Structures of model oligosaccharides used in this study: (A) PA-labeled Le^x-pentasaccharide (oligosaccharide I); (B) PA-labeled Le^a-pentasaccharide (oligosaccharide II); and (C) PA-labeled Le^x-asialotriantennary complex type oligosaccharide (oligosaccharide III).

nanoESI-MS^n

Experiments were performed using a Finnigan linear ion trap Fourier transform ion cyclotron resonance mass spectrometer (LTQ-FT, ThermoElectron, San Jose, CA, USA) equipped with a nanoESI source (AMR, Inc., Tokyo, Japan). ESI-MS^n was carried out for Le^x- and Le^a-oligosaccharide standards at a concentration of 1 pmol/μL in 5 mM ammonium acetate and 10 μM NaCl buffer (pH 9.6) containing 50% acetonitrile. The sample was analyzed at a flow rate of 2.0 μL/min using a spray voltage of 2.0 kV in the positive ion mode. The capillary temperature was set to 200°C; collision energies were set to 20–30% for the MS^n experiments; the maximum scan time was set to 50 ms. MS^2 and MS^3 were performed with an isolation width of 3.0 u (range of precursor ion ±1.5).

LC/MS^n

LC was carried out using a MAGIC 2002 system (Michrom BioResources, Auburn, CA, USA) equipped with a GCC (Hypercarb column, 150 × 0.2 mm, ThermoElectron). The

eluents were 5 mM ammonium acetate, pH 9.6, containing 2% acetonitrile (pump A) and 5 mM ammonium acetate, pH 9.6, containing 80% acetonitrile (pump B). PA-labeled *N*-linked oligosaccharides from murine kidney were eluted at a flow rate of 2 μL/min with a gradient of 10–70% of pump B in 60 min. A solution of NaCl (10 μM) was passed post-column at a flow rate of 2 μL/min. The precursor ions detected by a full MS^1 scan (mass range at *m/z* 750–2000) were followed by MS^2 scans of the most intense ions.

RESULTS AND DISCUSSION

MS^n of Le^x-pentaoligosaccharide

The model Le^x-pentaoligosaccharide (oligosaccharide I) was analyzed by nanoESI-MS^n with direct injection in the positive ion mode. Sodium chloride (NaCl) was deliberately added to the sample for the acceleration of the cross-ring cleavages according to previous reports.[22–24] The sodiated singly charged molecular ion, $[M+Na]^+$, of oligosaccharide I was observed at *m/z* 954.4 in the MS^1 spectrum (Fig. 3(A)). MS^2 of the sodiated molecular ion yielded $[(M+Na)\text{-Fuc}]^+$ at *m/z* 808 as the most intense ion by the glycosidic bond cleavage between GlcNAc and Fuc residues (Fig. 3(B)). This indicates that the Fuc residue is easily dissociated by low-energy CID MS^2. In addition to the defucosylated ions, we observed the sodiated ion at *m/z* 534, corresponding to the Le^x and Le^a structure, $[Gal(Fuc)GlcNAc+Na]^+$. The sodiated B_2 ion (*m/z* 534) was subjected to a further product ion scan, and the sodiated ion at *m/z* 388 corresponding to $[GalGlcNAc+Na]^+$ appeared in the MS^3 spectrum (Fig. 3(C)). The ion at *m/z* 372, corresponding to $[FucGlcNAc+Na]^+$, which proves the attachment of Fuc to GlcNAc, was also detected. Then, MS^4 of the sodiated $Y_{3\alpha}$ ion (*m/z* 388) yielded a sodiated cross-ring fragment ion at *m/z* 259, corresponding to the sodiated $^{3,5}A_2$ ion, which proves the linkage of the Gal residue at position C-4 on GlcNAc, with some neutral losses: 60 Da ($^{0,4}A_2$, $^{0,4}X_{4\beta}$, $^{1,3}X_{4\beta}$ and $^{2,4}X_{4\beta}$) and 90 Da ($^{0,3}X_{4\beta}$ and $^{1,4}X_{4\beta}$) (Fig. 3(D)).

MS^n of Le^a-pentaoligosaccharide

The Le^a-pentasaccharide (oligosaccharide II) was subjected to nanoESI-MS^n in a similar manner. The $[M+Na]^+$ of oligosaccharide II was observed at *m/z* 954.4 in the MS^1 spectrum (Fig. 4(A)). MS^2 of the $[M+Na]^+$ at *m/z* 954 yielded the sodiated ion at *m/z* 534, corresponding to $[Gal(Fuc)GlcNAc+Na]^+$ (Fig. 4(B)). MS^3 of the sodiated B_2 ion (*m/z* 534) yielded the sodiated $Y_{3\alpha}$ and $Y_{3\beta}$ ions at *m/z* 372 and 388, respectively (Fig. 4(C)). MS^4 of the sodiated $Y_{3\beta}$ ion at *m/z* 388 yielded some cross-ring fragment ions at *m/z* 208, 268, 298 and 328, corresponding to neutral losses: 60 Da ($^{0,4}A_2$, $^{0,4}X_{4\beta}$, $^{1,3}X_{4\beta}$ and $^{2,4}X_{4\beta}$) and 90 Da ($^{0,3}A_2$, $^{0,3}X_{4\beta}$ and $^{1,4}X_{4\beta}$) (Fig. 4(D)). $^{3,5}A_2$ at *m/z* 259, which arose from oligosaccharide I, was not detected by MS^4 of Le^a.

These results suggest that the Le^x structure can be identified by the $^{3,5}A_2$ ion at *m/z* 259 generated by MS^4 of $[GalGlcNAc+Na]^+$ at *m/z* 388, which arose from MS^3 $[Gal(Fuc)GlcNAc+Na]^+$ at *m/z* 534 (Fig. 5).

MS^n of Le^x-asialotriantennary oligosaccharide

Using a Le^x-oligosaccharide with a more complicated branching structure, we confirmed the practicability of MS^3 of the ion at *m/z* 534 followed by MS^4 of the ion at *m/z* 388 for the detection of the Le^x-diagnostic ion at *m/z* 259.

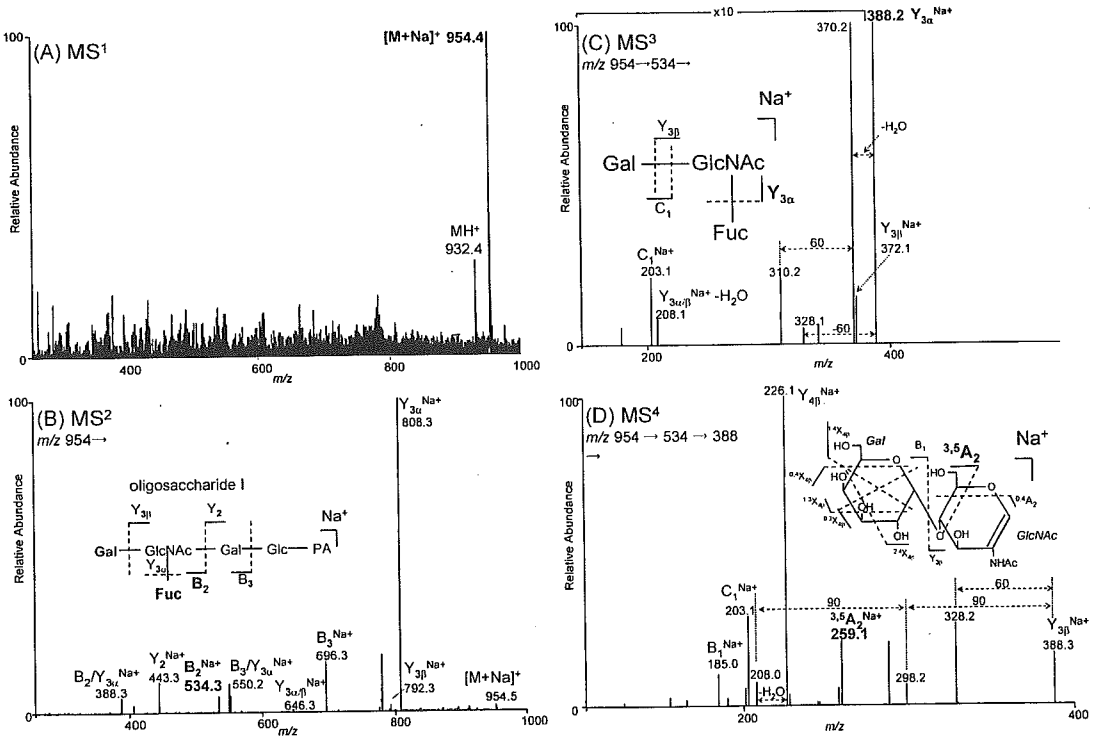

Figure 3. MS$^{1-4}$ spectra of oligosaccharide I by ESI-MS^n: (A) MS^1 spectrum; (B) MS^2 spectrum of $[M+Na]^+$ at *m/z* 954.4; (C) MS^3 spectrum of $[Gal(Fuc)GlcNAc+Na]^+$ at *m/z* 534.3 detected in MS^2; and (D) MS^4 spectrum of $[GalGlcNAc+Na]^+$ at *m/z* 388.2 detected in MS^3.

RCM

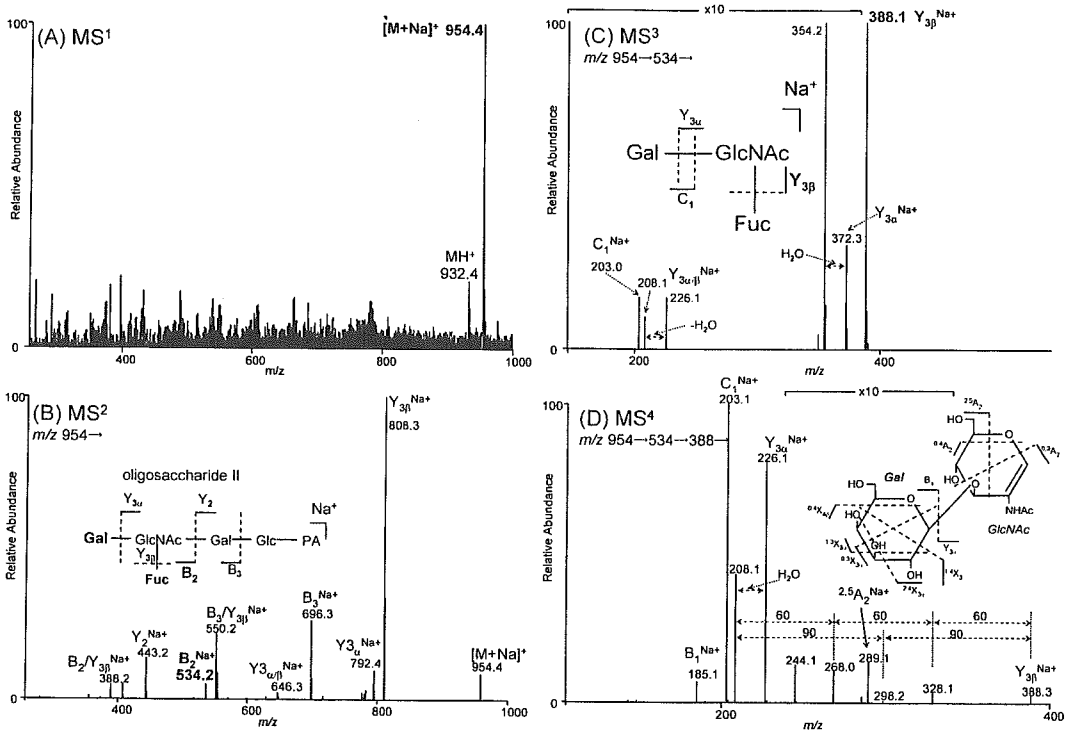

Figure 4. MS^{1-4} spectra of oligosaccharide II by ESI-MS^n: (A) MS^1 spectrum; (B) MS^2 spectrum of $[M+Na]^+$ at *m/z* 954.4; (C) MS^3 spectrum of $[Gal(Fuc)GlcNAc+Na]^+$ at *m/z* 534.2 detected in MS^2; and (D) MS^4 spectrum of $[GalGlcNAc+Na]^+$ at *m/z* 388.1 detected in MS^3.

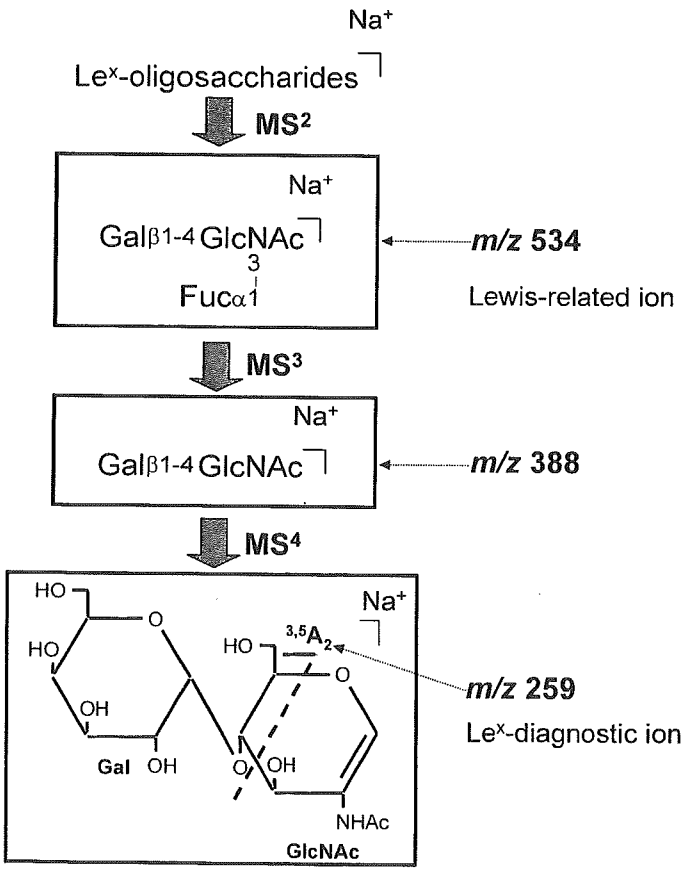

Figure 5. Proposed method for the Le^x-specific detection by ESI-MS^n.

Figure 6 shows the MS^{2-4} spectra of Le^x-asialotriantennary (oligosaccharide III). The oligosaccharide sequence can be confirmed by product ions generated by MS^2 (Fig. 6(A)). In addition to the defucosylated ion, many B- and Y-series ions, including the sodiated ion at *m/z* 534 corresponding to $[Gal(Fuc)GlcNAc+Na]^+$, were generated by MS^2. MS^3 of the sodiated $B_{2\alpha'}$ ion at *m/z* 534 yielded the sodiated $Y_{5\alpha''}$ ion at *m/z* 388 as the most intense ion (Fig. 6(B)). MS^4 of the $Y_{5\alpha''}$ ion at *m/z* 388 predictably generated the $^{3,5}A_2$ ion (*m/z* 259) (Fig. 6(C)). These results indicate that MS^3 of the sodiated ion at *m/z* 534, followed by MS^4 of the sodiated ion at *m/z* 388, can be used for the detection of the Le^x-diagnostic motif even in large and complicated *N*-linked oligosaccharides.

Specific detection and structural elucidation of *N*-linked Le^x-oligosaccharides in murine kidney by LC/ESI-MS^n

A sequential scan consisting of a full MS^1 scan, data-dependent MS^2 scan, MS^3 scan of the ion at *m/z* 534, and MS^4 scan of the ion at *m/z* 388 was applied to the specific detection and structural elucidation of Le^x-oligosaccharides in the murine kidney. In order to separate the many different oligosaccharides, including isomers, we used a LC/ITMS system equipped with a GCC. The *N*-linked oligosaccharides were released by PNGase F from the carboxymethylated proteins in the murine kidney soluble fraction. To improve the ionization efficiency and sensitivity,[25,26] the oligosaccharides were pyridylaminated, and the PA-oligosaccharides were subjected to LC/ESI-MS^n with a sequential scan. Sodiated ions were generated by a post-column reaction with 10 μM NaCl solution (2 μL/min). Oligosaccharides that yielded the

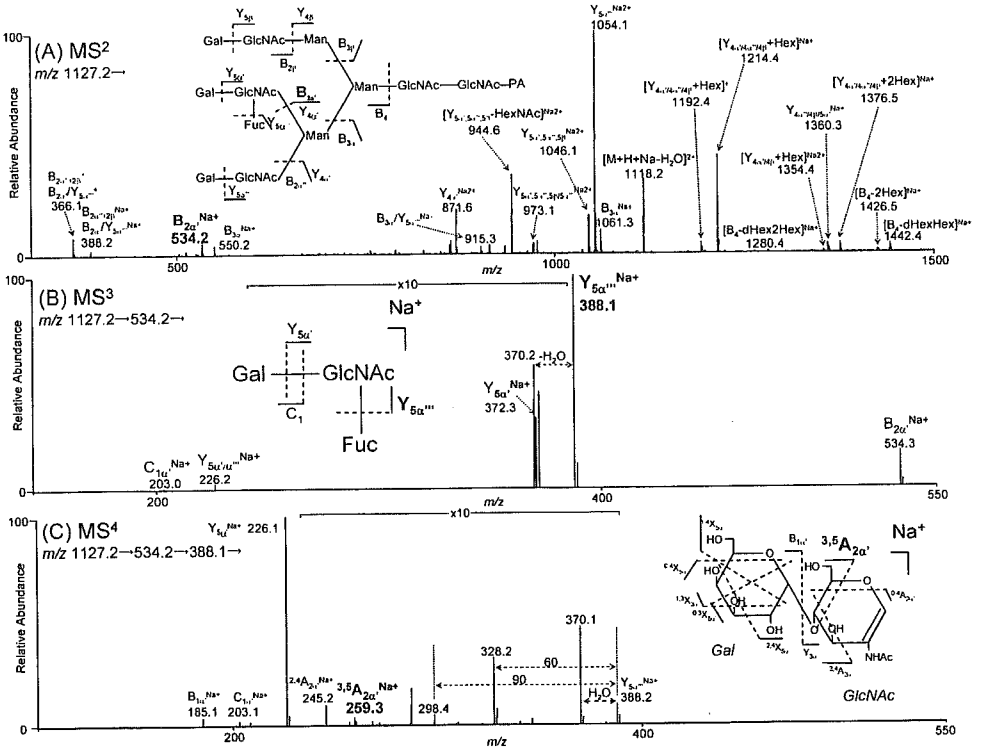

Figure 6. MS$^{2-4}$ spectra of oligosaccharide III by ESI-MS^n: (A) MS^2 spectrum of $[M+H+Na]^{2+}$ at *m/z* 1127.2; (B) MS^3 spectrum of $[Gal(Fuc)GlcNAc+Na]^+$ at *m/z* 534.2 detected in MS^2; and (C) MS^4 spectrum of $[GalGlcNAc+Na]^+$ at *m/z* 388.1 detected in MS^3.

diagnostic ions by MS$^{1-4}$ scans were presumed to be those of Le^x-oligosaccharides, and their detailed structures were elucidated by their data-dependent MS^2 spectra.

Figure 7(A) shows the total ion current (TIC) profile obtained by the full MS^1 scan of PA-labeled oligosaccharides from the murine kidney. Structures of major oligosaccharides a–i were deduced from the masses of the sodiated molecular ions measured by FTMS together with the B/Y ions generated by CID MS^2 (Table 1). Figures 7(B)–7(D) show mass chromatograms at *m/z* 534, 388 and 259, respectively, detected by MS$^{2-4}$, respectively. These chromatograms revealed that at least five kinds of oligosaccharides contain the Le^x-motif (a, b, e, f and h). Based on the masses, they were assigned to fucosylated oligosaccharides consisting of $dHex_3Hex_5HexNAc_5$ (a and f), $dHex_2Hex_5HexNAc_5$ (b), $dHexHex_4HexNAc_5$ (e), and $dHex_2Hex_4HexNAc_5$ (h) (abbreviations used here are: dHex, deoxyhexose; Hex, hexose; HexNAc, *N*-acetylhexosamine).

As an example of structural elucidation, we show the MS$^{2-4}$ spectra of oligosaccharide f in Fig. 8. In the MS^2 spectrum, we can observe the product ion $[dHex_2HexHexNAc+Na]^+$ at *m/z* 680, which can be assigned to either the Lewis b (Le^b)- or Lewis y (Le^y)-motif. As shown in Fig. 1, Le^b- and Le^y-motifs contain Le^a and Le^x as partial structures, respectively. The generation of Le^x-diagnostic ions suggests the attachment of the Le^y-motif to oligosaccharide f. Furthermore, product ions at *m/z* 1036 and 446 prove the linkage of GlcNAc at *β*-mannose in the trimannosyl core structure and fucosylation of the reducing terminal GlcNAc, respectively. Based on these characteristic ions, oligosaccharide f can be assigned to the bisected and fucosylated biantennary bearing the

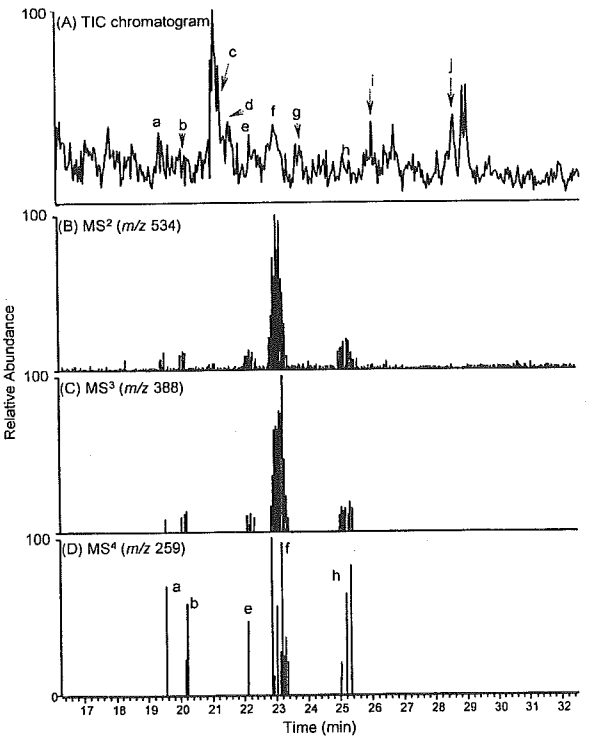

Figure 7. Specific detection of *N*-linked Le^x-oligosaccharides in murine kidney by LC/ESI-MS^n: (A) total ion chromatogram obtained by MS^1; (B) mass chromatogram of $[dHexHexNAc+Na]^+$ at *m/z* 534 detected in MS^2; (C) mass chromatogram of $[HexHexNAc+Na]^+$ at *m/z* 388 detected in MS^3; and (D) mass chromatogram of the cross-ring fragment at *m/z* 259 detected in MS^4.

Table 1. Sugar composition and deduced structure of *N*-linked oligosaccharide from murine kidney

Sugar No.	Composition[a]	Deduced structure	Lewis type
a	$dHex_3Hex_5HexNAc_5$		Le^y
b	$dHex_2Hex_5HexNAc_5$		Le^x
c	$Hex_8HexNAc_2$		
d	$Hex_9HexNAc_2$		
e	$dHexHex_4HexNAc_5$		Le^x
f	$dHex_3Hex_5HexNAc_5$		Le^y
g	$Hex_6HexNAc_2$		
h	$dHex_2Hex_4HexNAc_5$		Le^x
i	$Hex_7HexNAc_2$		
j	$Hex_5HexNAc_2$		

[a]Fuc, fucose; Hex, hexose; HexNAc, *N*-acetylhexosamine.
○ Gal; ○ Man; ■ GlcNAc; △ Fuc.

Le^y-motif. The Le^y structure in oligosaccharide f was confirmed by an extra LC/MS^2 run without post-column reaction with NaCl. Figure 9 shows the MS^2 spectrum of $[M+H+NH_4]^{2+}$ at *m/z* 1189.4. Attachment of the Le^y-motif was proved by the generation of the product ion at *m/z* 658 corresponding to $[dHex_2HexHexNAc]^+$.

Other oligosaccharides were assigned to bisected biantennary forms bearing Le^y (oligosaccharide a) and those bearing Le^x (oligosaccharides b, e and h) motifs. In addition to the previously reported Le^x-oligosaccharides,[20] we also detected the presence of Le^y-oligosaccharides in the murine kidney.

CONCLUSIONS

We found that the cross-ring fragment ion at *m/z* 259, which can be used for distinction from positional isomers, was generated from Le^x-oligosaccharides by MS^4 of $[GalGlcNAc+Na]^+$ at *m/z* 388, which was generated by MS^3 of $[Gal(Fuc)GlcNAc+Na]^+$ at *m/z* 534. Then, we successfully detected and elucidated the Le^x- and Le^y-oligosaccharides in the complex mixture using a sequential scan consisting of full MS^1, data-dependent MS^2, MS^3 of the sodiated ion at *m/z* 534, and MS^4 of the sodiated ion at *m/z* 388.

The Le^x structure is associated with various biological events as oligosaccharide ligands. So far, the detection and structural analyses of Le^x-oligosaccharides have required complicated and time-consuming processes, such as exoglycosidase digestions, sugar mapping,[27] the use of lectins and immunological methods. The mass spectrometric method proposed here would enable the rapid and easy detection of the Le^x-motif and subsequent structural elucidation of

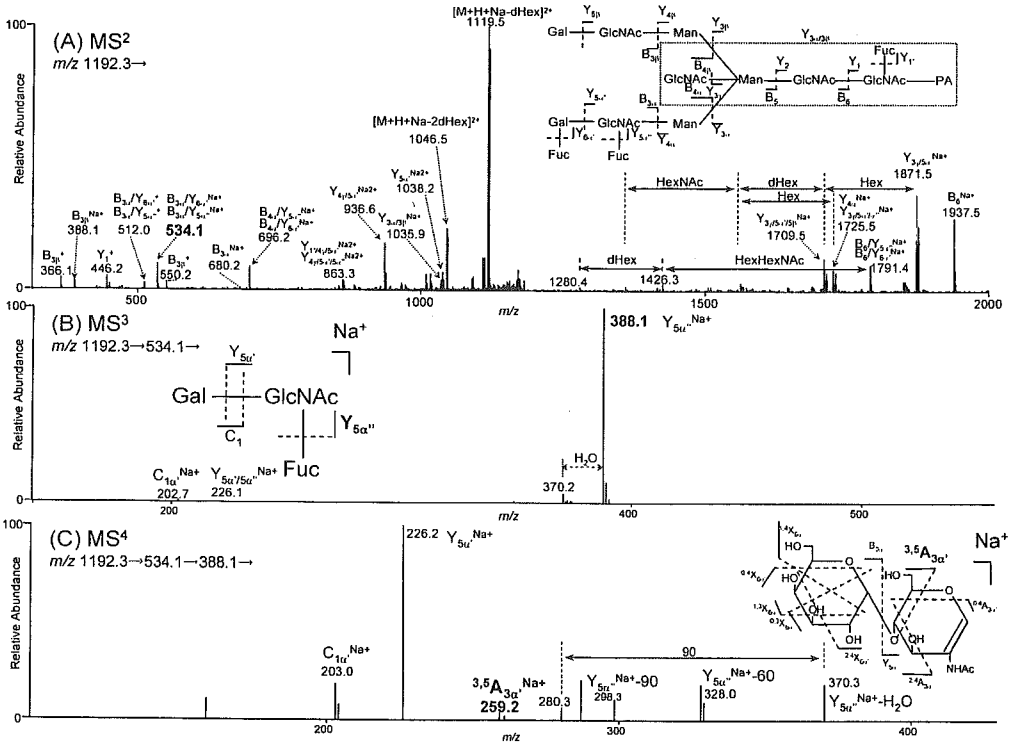

Figure 8. MS^{2-4} spectra of oligosaccharide f by LC/ESI-MS^n: (A) MS^2 spectrum of $[M+H+Na]^{2+}$ at *m/z* 1192.3; (B) MS^3 spectrum of $[dHexHexNAc+Na]^+$ at *m/z* 534.1 detected in MS^2; and (C) MS^4 spectrum of $[HexHexNAc+Na]^+$ at *m/z* 388.1 detected in MS^3.

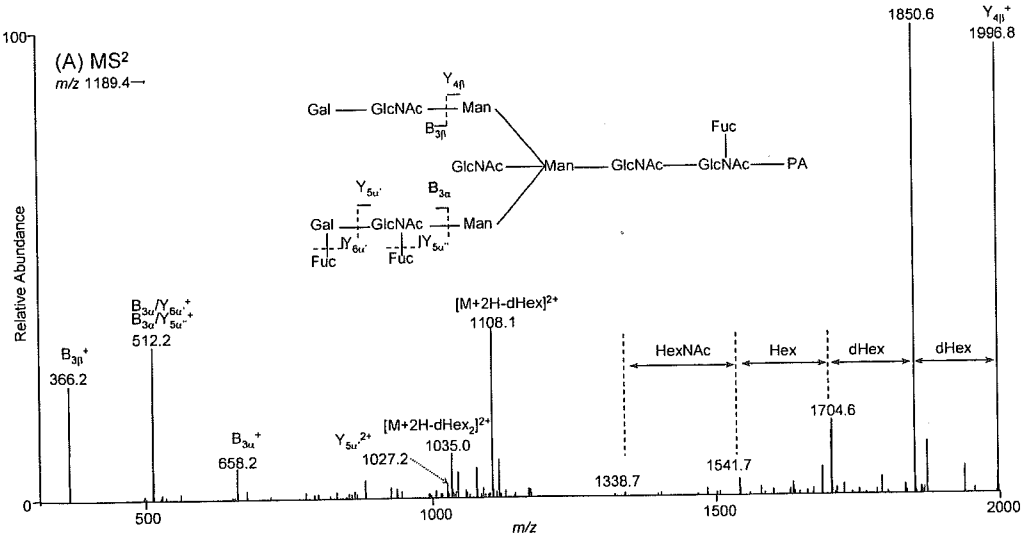

Figure 9. MS^2 spectrum of oligosaccharide f by LC/ESI-MS^n: precursor ion, $[M+H+NH_4]^{2+}$ at *m/z* 1189.9.

Le^x-oligosaccharides in biological samples. Our method, based on a sequential scan for the structure-characteristic ions, may be applicable to the analyses of oligosaccharides carrying other partial motifs, such as sialyl Le^x and sulfated sugar.

Acknowledgements

This study was supported in part by Grant-in-Aid from the Ministry of Health Labor and Welfare, and Core Research for the Evolutional Science and Technology Program, Japan Science and Technology Corp.

REFERENCES

1. Feizi T. *Nature* 1985; **314**: 53.
2. Walz G, Aruffo A, Kolanus W, Bevilacqua M, Seed B. *Science* 1990; **250**: 1132.
3. Kannagi R, Izawa M, Koike T, Miyazaki K, Kimura N. *Cancer Sci.* 2004; **95**: 377.
4. Coombs PJ, Graham SA, Drickamer K, Taylor ME. *J. Biol. Chem.* 2005; **280**: 22993.
5. Larkin M, Ahern TJ, Stoll MS, *et al. J. Biol Chem.* 1992; **267**: 13661.
6. Lowe JB, Stoolman LM, Nair RP, Larsen RD, Berhend TL, Marks RM. *Cell* 1990; **63**: 475.
7. Phillips ML, Nudelman E, Gaeta FC, Perez M, Singhal AK, Hakomori S, Paulson JC. *Science* 1990; **250**: 1130.
8. Sagi D, Peter-Katalinic J, Conradt HS, Nimtz M. *J. Am. Soc. Mass Spectrom.* 2002; **13**: 1138.
9. Sheeley DM, Reinhold VN. *Anal. Chem.* 1998; **70**: 3053.
10. Xue J, Song L, Khaja SD, Locke RD, West CM, Laine RA, Matta KL. *Rapid Commun. Mass Spectrom.* 2004; **18**: 1947.
11. Karlsson NG, Schulz BL, Packer NH. *J. Am. Soc. Mass Spectrom.* 2004; **15**: 659.
12. Karlsson NG, Wilson NL, Wirth HJ, Dawes P, Joshi H, Packer NH. *Rapid Commun. Mass Spectrom.* 2004; **18**: 2282.
13. Zhang S, Chelius D. *J. Biomol. Technol.* 2004; **15**: 120.
14. Royle L, Mattu TS, Hart E, Langridge JI, Merry AH, Murphy N, Harvey DJ, Dwek RA, Rudd PM. *Anal. Biochem.* 2002; **304**: 70.
15. Takegawa Y, Deguchi K, Ito S, Yoshioka S, Nakagawa H, Nishimura S. *Rapid Commun. Mass Spectrom.* 2005; **19**: 937.
16. Takegawa Y, Ito S, Yoshioka S, Deguchi K, Nakagawa H, Monde K, Nishimura S. *Rapid Commun. Mass Spectrom.* 2004; **18**: 385.
17. Mechref Y, Novotny MV, Krishnan C. *Anal Chem.* 2003; **75**: 4895.
18. Weiskopf AS, Vouros P, Harvey DJ. *Anal. Chem.* 1998; **70**: 4441.
19. Meisen I, Peter-Katalinic J, Muthing J. *Anal. Chem.* 2003; **75**: 5719.
20. Chui D, Sellakumar G, Green R, Sutton-Smith M, McQuistan T, Marek K, Morris H, Dell A, Marth J. *Proc. Natl. Acad. Sci. USA* 2001; **98**: 1142.
21. Yuan J, Hashii N, Kawasaki N, Itoh S, Kawanishi T, Hayakawa T. *J. Chromatogr. A* 2005; **1067**: 145.
22. Song F, Cui M, Liu Z, Yu B, Liu S. *Rapid Commun. Mass Spectrom.* 2004; **18**: 2241.
23. Cui M, Song F, Liu Z, Liu S. *Rapid Commun. Mass Spectrom.* 2001; **15**: 586.
24. Vakhrushev SY, Zamfir A, Peter-Katalinic J. *J. Am. Soc. Mass Spectrom.* 2004; **15**: 1863.
25. Suzuki S, Kakehi K, Honda S. *Anal. Chem.* 1996; **68**: 2073.
26. Yoshino K, Takao T, Murata H, Shimonishi Y. *Anal. Chem.* 1995; **67**: 4028.
27. Tomiya N, Awaya J, Kurono M, Endo S, Arata Y, Takahashi N. *Anal Biochem.* 1988; **171**: 73.

臨床化学　34：309－318，2005

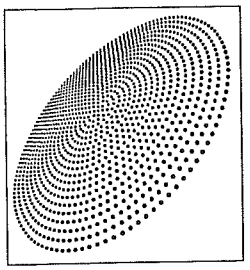

特集●Vol.34 No.4 微量糖鎖分析の現状と将来

LC/MSを用いたグライコーム解析

川崎ナナ*,**　橋井則貴*,**
伊藤さつき*　原園　景*　川西　徹*

Key words：LC/MS、グライコーム、グライコミクス、糖タンパク質、糖ペプチド、糖鎖

はじめに

細胞・組織に発現している全タンパク質（プロテオーム）を系統的・網羅的に解析することによって生命現象を解き明かそうとするプロテオミクスに高い関心が集まっている[1]。さらに最近では、細胞内タンパク質の主な翻訳後修飾の一つである糖鎖が、タンパク質の機能調節等を介して様々な疾患や発生・分化等に深く関わっていることが明らかになってきたことから[2-8]、細胞・組織発現糖タンパク質やその糖鎖部分の構造・機能を解析しようとするグライコミクスへの関心も高まっている[9,10]。

プロテオミクスの基盤的技術である質量分析法（MS）は、グライコミクスにおいても、糖タンパク質や糖鎖の構造特性解析のための有用なツールとして期待されている[11,12]。しかし、糖タンパク質は複数の糖鎖結合部位に様々な糖鎖が結合した不均一な集合体であることや、糖鎖が結合することによってMSにおけるイオン化効率が低下するなどの問題があるため、プロテオミクスの手法をそのまま利用できない場合が多い。そこで、レクチンや各種液体クロマトグラフィー（LC）など、糖鎖生物学分野で従来から利用されてきた糖鎖構造解析技術と、MSやデータベースを中心としたプロテオミクスの技術を組み合わせた様々なグライコーム解析技術の開発が進められている[13,14]。中でもLCとMSをオンラインで結んだLC/MSは、イオン化を妨害する物質を除去したり、不均一な糖鎖混合物を分離しながら、直接質量分析を行うことが可能な分析技術で、簡便・迅速なグライコーム解析法として優れている。本稿では、LC/MSを利用したグライコーム解析例をいくつか紹介する。

1. LC/MSによる細胞糖鎖の解析

疾患や発生・分化等に伴う糖鎖構造や糖鎖分布の微細な変化を見つけ出すには、糖タン

*国立医薬品食品衛生研究所生物薬品部
**独立行政法人科学技術振興機構（JST）戦略的創造研究推進事業（CREST）

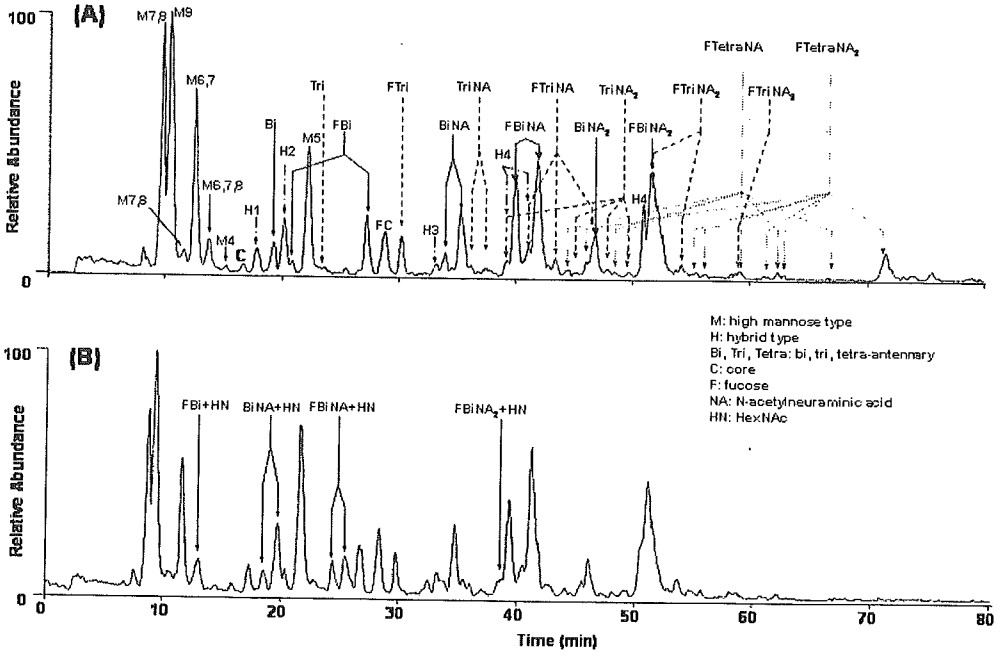

図1 (A) CH O細胞、及び(B) GnT-III遺伝子導入CHO細胞の糖鎖プロファイル

サンプル：CHO細胞(1 x 10^7) 膜画分から*N*-グリカナーゼによって切り出した糖鎖を$NaBH_4$で還元した
LC/MS：カラム，グラファイトカーボンカラム (0.2 x 150 mm)；溶離液A, 5 mM 酢酸アンモニウム/2 % アセトニトリル；溶離液B, 5 mM 酢酸アンモニウム/80 %アセトニトリル；グラジエント，B液 10-45 % (90 分)；流速，2 μl/min；MS, TSQ-7000 (サーモエレクトロン)

パク質から切り出した糖鎖を LC/MS を用いて解析する糖鎖プロファイリングが適している。構造糖鎖生物学分野ではこれまでに、糖鎖誘導体化とLCを組み合わせた様々な分離技術が開発されている[15-17]。これらをオンライン MS と組み合わせることによって、糖鎖不均一性の高い試料の解析が容易になる[18, 19]。筆者らは、糖タンパク質から*N*結合型糖鎖を酵素的に切り出し、還元末端を $NaBH_4$ で還元した後、親水性物質に対する吸着能の高いグラファイトカーボンカラムを用いて LC/MS (GCC-LC/MS) を行う糖鎖プロファイリング法を開発している[20-23]。以下に GCC-LC/MS を用いて細胞発現糖タンパク質の糖鎖を解析した例を2つ紹介する。

1.1 糖鎖プロファイリング

図1A は CHO 細胞の膜画分から*N*結合型糖鎖を酵素的に切り出した後、$NaBH_4$ で還元し、GCC-LC/MS 操置で分析して得られた結果をトータルイオンクロマトグラム (TIC) として表したもので、糖鎖の分布 (プロファイル) を示している。各ピークの糖鎖構造は、MS によって測定された質量を基に推定された単糖組成より、高マンノース型、及び2本鎖を中心とした複合型シアロ糖鎖であると推定された[24]。**図1B** は、CHO細胞に *N*-アセチルグルコサミン転移酵素 Ⅲ (GnT-Ⅲ) 遺伝子を導入した CHO 細胞の糖鎖プロファイルである。GnT-Ⅲ はトリマンノシルコアの β1-4Man に GlcNAc を付加させる酵素である。GnT-Ⅲ が導入された細胞には複数の新しい糖鎖が出現していることがわかる。これらは質量から、CHO 細胞に結合している 2本鎖糖鎖に *N*-アセチルヘキソサミン (HexNAc) が1分子 (203Da) 付加した糖鎖であることが確認され、GnT-Ⅲ によって生じた GlcNAc 付加糖鎖と推定された。このように糖鎖プロファイリングは、サンプル間の糖鎖の構造や分布を比較する方法として優れ、糖鎖生合成経路に起きた変化や、その変化に伴って生じた糖鎖の構造解析に利用できると期待される。

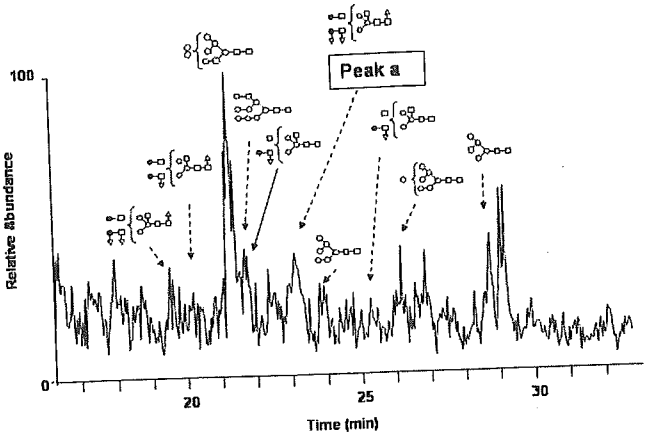

図2　マウス腎臓の糖鎖プロファイル

サンプル：腎臓(20 μgタンパク質)の膜を含む画分から*N*-グリカナーゼによって切り出した糖鎖を$NaBH_4$で還元した
LC/MS：カラム及び溶離液，図1に準ずる；グラジエント，B液 5-45 %（60 分）；流速，2 μl/min；MS，LTQ (サーモエレクトロン)
●，Gal；○，Man；□，GalNAc；△，Fuc

1.2　糖鎖配列解析

糖鎖の配列や結合様式は、MS を繰り返す多段階 MS (MS^n) によって、ある程度決定することができる[25-27]。**図2** は、マウス腎臓の膜画分から切り出した *N*結合型糖鎖を 2-アミノピリジンで誘導体化し、LC/MS による糖鎖プロファイリングを行ったものである。主な糖鎖は質量から、高マンノース型糖鎖、及び複数のフコースが結合した複合型糖鎖と推定された。各糖鎖の配列は、MS^n により決定した[28]。一例として、**図3** にフコシル糖鎖ピーク a の MS^{2-4} スペクトルを示す。MS^2 によって [ヘキソース(Hex)-HexNAc-Fuc + Na]$^+$ (*m/z* 534)、及び [Hex-HexNAc-Fuc_2 + Na]$^+$ (*m/z* 680) が生じたことから、ピーク a にはルイス b (Le^b, Fucα 1-2Galβ 1-3(Fucα 1-4)GlcNAc)、またはその異性体ルイス y (Le^y, Fucα 1-2Galβ 1-4(Fucα 1-3)GlcNAc) 構造が存在することが示唆された(**図3A**)。そこで、*m/z* 534 を前駆イオンとし

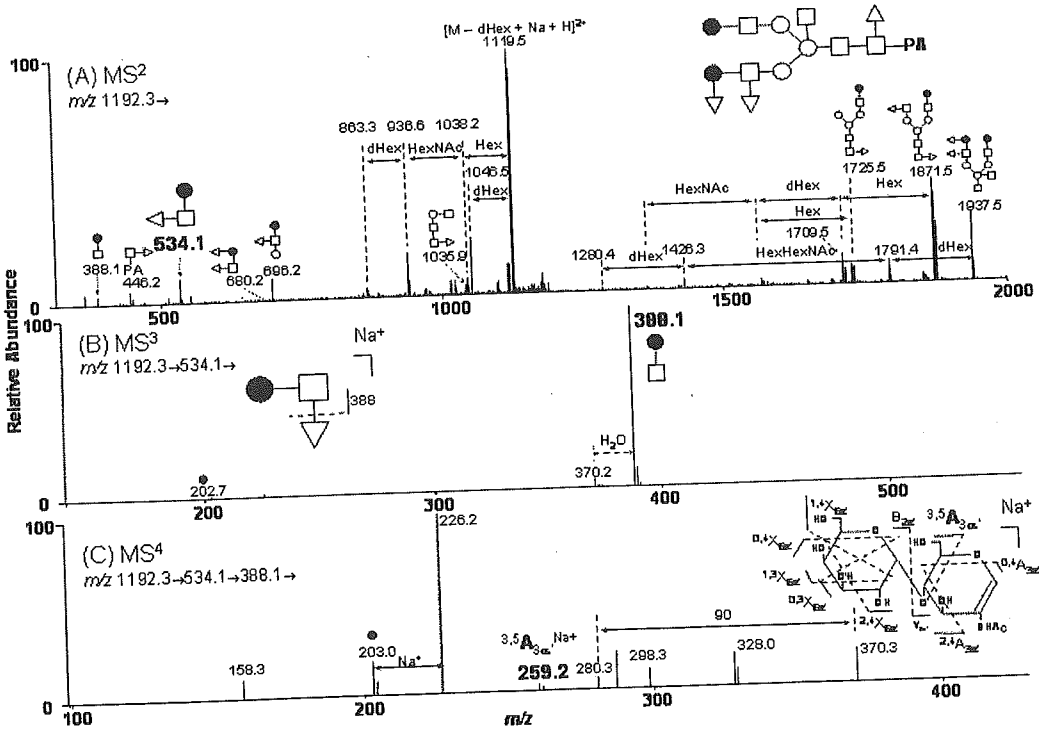

図3　図2中のピークaの（A） MS^2 （前駆イオン：*m/z* 1192.3）、（B） MS^3 （前駆イオン：*m/z* 534）、及び（C） MS^4（前駆イオン：*m/z* 388）スペクトル

て MS^3 を行ったところ、フコースが開裂した $[Hex\text{-}HexNAc + Na]^+$ (m/z 388) が検出された(**図3B**)。つぎに m/z 388 を前駆イオンとして MS^4 を行ったところ、環開裂した GlcNAc の4位炭素原子に Gal が結合したイオン (m/z 259) が検出されたことから、この部分構造は Le^y と決定された(**図3C**)。さらに、他の糖鎖のプロダクトイオンを解析した結果、マウス腎臓に結合しているフコシル糖鎖は Le^x 及び Le^y 糖鎖であることが明らかとなった。Le^x は SSEA-1 糖鎖としても知られる糖鎖エピトープで、マウス ES 細胞に多く発現していることが知られ、ES 細胞の分化状態のモニタリングに利用されている糖鎖である[29]。また、シアル酸が結合したシアリル Le^x はヒト腫瘍マーカーとして利用されており[30]、マウス腎臓の主な糖鎖が Le^x 糖鎖であったことは興味深い。

2. LC/MSによる糖ペプチド解析

タンパク質から糖鎖を切り離すと、糖鎖とタンパク質間の結合に関する情報が失われてしまうので、細胞・組織中の任意の糖タンパク質糖鎖の構造特性解析は糖鎖を切り離さずに行う。膜糖タンパク質などは不溶性または高分子量タンパク質であることが多いので、還元アルキル化した後、トリプシン、Lys-C、Glu-C、または Asp-N 等で消化してから分析するのが一般的である。MS において、ペプチドに比べて糖ペプチドのイオン化効率が悪いために、ペプチドが混在すると糖ペプチドのマススペクトルが得られにくいという問題があるが、LC/MS によってペプチドを除きながら質量測定を行えば、良好な糖ペプチドのマススペクトルを得ることができる[31-33]。糖タンパク質消化物の LC/MS では複雑なクロマトグラムが得られることが多いが、MS^n やインソースフラグメンテーションによって生じた糖鎖に特徴的なイオン、例えば、$HexNAc^+$ (m/z 204) や $Hex\text{-}HexNAc^+$ (m/z 366) などを利用することによって、糖ペプチドの MS^2 スペクトルを選び出すことができる[32, 34]。選び出した糖ペプチドの MS^2 スペクトルには、ペプチドやペプチドに GlcNAc が結合したイオンが検出されている場合が多く、これらのイオンを基にペプチドと糖鎖部分の構造を決定する[32, 33]。

2.1 糖タンパク質の網羅的解析

図4A は、アルブミンをある程度除去したヒト血清のトリプシン消化物 0.02 μl 相当を、C18カラムを用いた LC/MS^2 装置で分析して得られた MS^1 の TIC である。血清は様々なタンパク質の混合物であるので、非常に多くのペプチドが検出されているが、MS^2 によって生じた $HexNAc^+$ (m/z 204) を指標として、糖ペプチドのMS^2スペクトルを選び出した(**図4B**)。選び出した糖ペプチドのペプチド配列と糖鎖構造は、MS^2 スペクトルを基に決定した。一例として**図5** にピーク b の MS^2 スペクトルを示す。m/z 1442 に検出されている [ペプチド + GlcNAc + 2H]$^{2+}$、及びペプチド由来のフラグメント (b, yイオン) から、この糖ペプチドはハ

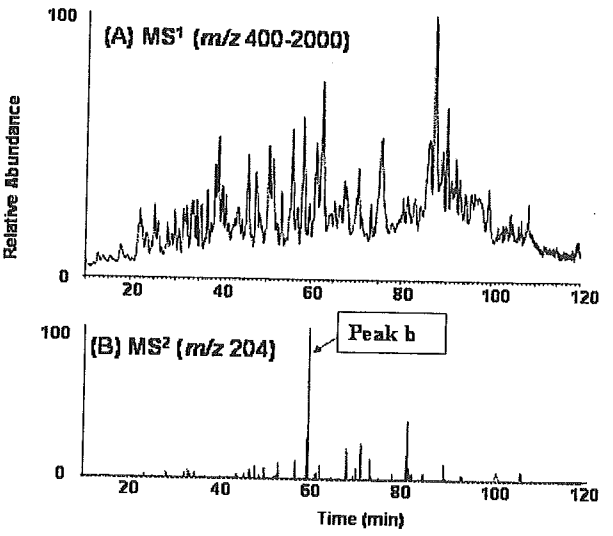

図4 (A) アルブミン除去ヒト血清トリプシン消化物のLC/MSによって得られたTIC、(B)LC/MS/MSによって生じたm/z 204イオンのマスクロマトグラム
LC/MS：カラム, C18 (0.2 x 50 mm); 溶離液A, 0.1 % ギ酸-2 %アセトニトリル; 溶離液B, 0.1 % ギ酸-90 %アセトニトリル; グラジエント, B液 5-50% (120 分)；流速, 2 μl/min; MS, QSTAR (アプライドバイオシステムズ)

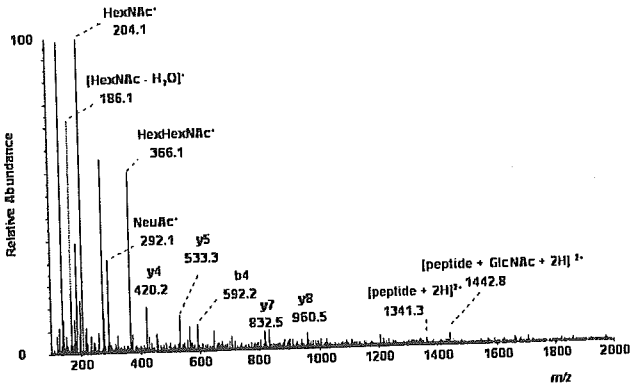

図5　図4B中のピークbのMS²スペクトル

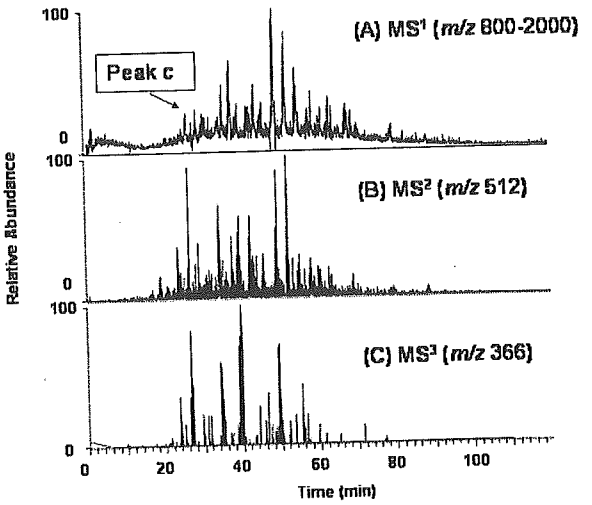

図6　(A)マウス腎臓トリプシン消化物由来フコシル糖ペプチドのTIC、(B)データ依存的MS²によって生じたm/z 512イオンのマスクロマトグラム、(C) MS³(前駆イオン：m/z 512)によって生じたm/z 366イオンのマスクロマトグラム

サンプル：マウス腎臓膜画分トリプシン消化物のAALアフィニティークロマトグラフィー吸着画分
LC/MS：カラム及び溶離液，図4に準ずる；MS，LTQ

プトグロビンの Met120-Lys143 と推定された。また、糖鎖構造は、糖ペプチドの分子量とペプチド部分の分子量の差からジシアロ２本鎖糖鎖と推定された。この方法により、ハプトグロビンの他、血清中のトランスフェリン由来糖ペプチドなども解析することができた。

2.2　糖鎖構造選択的糖タンパク質解析

ペプチド混合物の中からすべての糖ペプチドを選び出す場合は、糖鎖にほぼ共通して存在するHexNAc$^+$ を利用するが、任意の糖鎖を有する糖ペプチドのみを選び出す場合は、その構造に特徴的なイオンを利用する。例えば、マウス腎臓から前述した Le^x 結合ペプチドを見つけだす場合は、Le^x に相当する Hex-(Fuc)HexNAc$^+$ (*m/z* 512) 及び Hex-HexNAc$^+$ (*m/z* 366) を指標とすればよい。**図6** は、マウス腎臓膜画分をトリプシン消化し、フコースを認識する AAL レクチンアフィニティークロマトグラフィーによりフコシル糖ペプチドを回収した後、C18 カラムを用いて LC/MS^{2,3} を行った結果である。MS^1 では複雑なクロマトグラムが得られたが (**図6A**)、MS^2 によって Gal β1-4(Fuc α 1-3)GlcNAc$^+$ を生じ (**図6B**)、さらに MS^3 によって Gal β1-4GlcNAc$^+$ を生じたペプチドを Le^x 結合糖ペプチドとして選別した (**図6C**)。選び出した糖ペプチドの糖鎖構造は、別途、強度の高いイオンを前駆イオンとして自動的に MS^n を行うデータ依存的 MS^n によって解析した。**図7** はピーク c に溶出された Le^x 結合糖ペプチドのデータ依存的 MS^2 及び MS^3 スペクトルである。フラグメントパターンからこの糖ペプチドは、**図7** に示すような Le^x 部分構造を 2分子有する糖鎖であることが明らかになった。さらに、MS^2 で生じた [peptide + GlcNAc+ 2H]$^{2+}$ (*m/z* 906) を前駆イオンとして MS^3 を行った後、プロテオミクスで利用されているデータベース検索を行ったところ、この糖ペプチドはガンマーグルタミルトランスフェラーゼの LHNQLLPN*TTTVEK (*糖鎖結合位置) と推定された。マウスガンマーグルタミルトランスフェラーゼに Le^x 糖鎖が結合していることは、木幡らによって報告されている[35]。このように、これまでは糖タンパク質を特定してから糖鎖を解析するのが一般的であったが、LC/MS^n とタンパク質データベース検索を利用することによって、任意の糖鎖構造からタンパク質を特定することが可能となってきた。

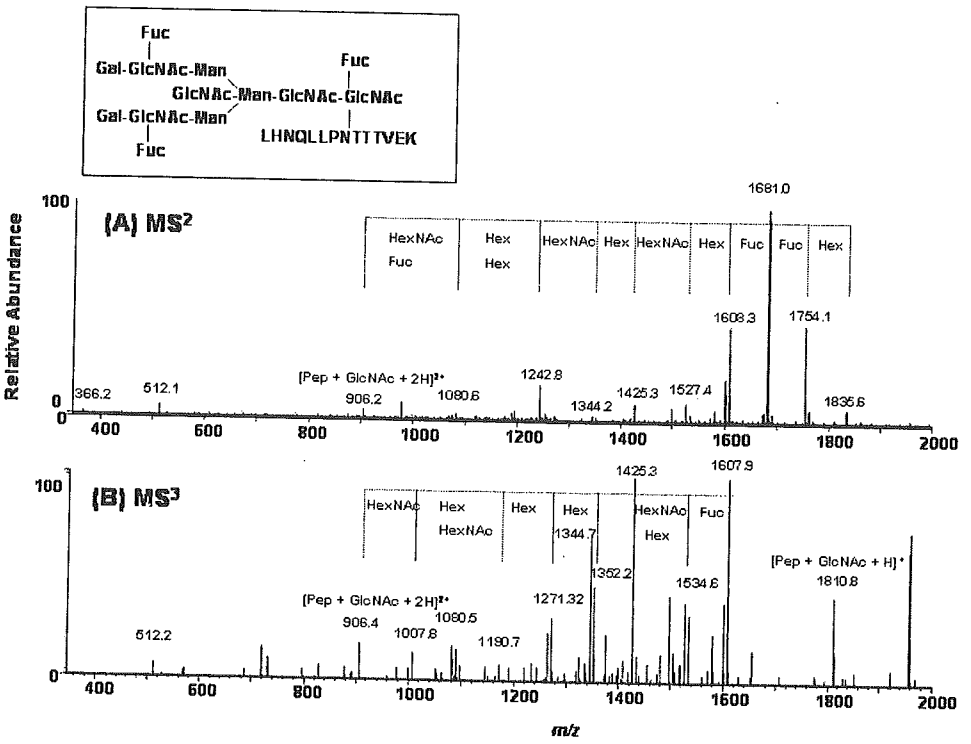

図7　図6中のピークcの位置に溶出された糖ペプチドの（A）データ依存的MS^2、及び（B）データ依存的MS^3スペクトル

3. 電気泳動法とLC/MSを用いた糖タンパク質の構造特性解析

細胞内糖タンパク質をインタクトのままで扱う場合は、不溶性糖タンパク質や、複雑な混合物中の糖タンパク質の分離に優れた電気泳動を利用するのが効果的である[36, 37]。電気泳動を利用したグライコーム解析例を2つ示す。

3.1 レクチンブロットとLC/MSによる糖タンパク質の同定

はじめに2次元電気泳動とレクチンを利用することによって、任意の糖鎖構造を持つコアタンパク質を特定した例を示す。**図8A**は、前述のGnT-Ⅲ遺伝子導入CHO細胞の2次元電気泳動図である。PHA-E_4レクチン染色を行い、GnT-ⅢによってGlcNAcが付加されたタンパク質の位置を特定した（**図8B**）。別に展開した泳動ゲルからレクチンで染まった位置に相当するスポットを切り出し、ゲル内トリプシン消化、ペプチド抽出、LC/MS、及びタンパク質データベース検索を行った結果、このタンパク質はインテグリンα3と同定された[24]。GnT-Ⅲは癌細胞転移抑制に関与していることが知られている酵素で[38-40]、そのターゲットタンパク質として細胞接着に関与しているインテグリンが同定されたのは興味深い[41]。

3.2 LC/MS^nによるゲル内糖タンパク質の構造特性解析

つぎに、LC/MSを利用してゲル内糖タンパク質の同定、及び部位特異的糖鎖解析を行った例を示す。**図9A**はマウス脳の膜画分から調製したGPIアンカー型タンパク質群をSDS-PAGEで展開し、クーマシー染色したものである。20-23kDaに表れているタンパク質は、SDSによる抽出、トリプシン消化、LC/MS^n（**図9B**）、及びデータベース検索の結果、免疫グロブリンスーパーファミリーに属するThy-1と同定された。**図9C**はインソースフラグメンテーションによって生じたm/z 204のイオンのマスクロマトグラムで、糖ペプチドの溶出位置を示している。各糖ペプチドの糖鎖と

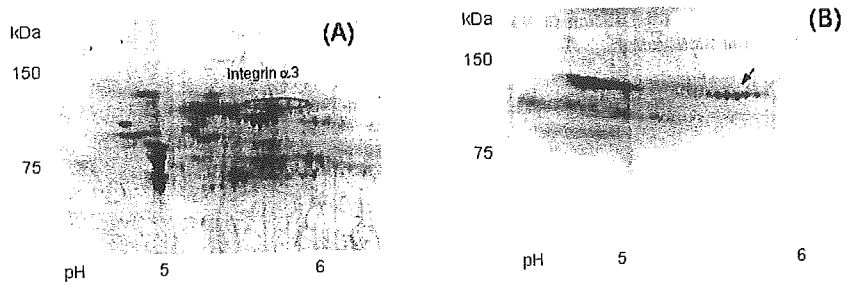

図8　GnT-III 遺伝子導入CHO 細胞の膜を含む画分の2次元電気泳動図
(A)CYPRO Orange 染色、(B)PHA-E_4レクチン染色

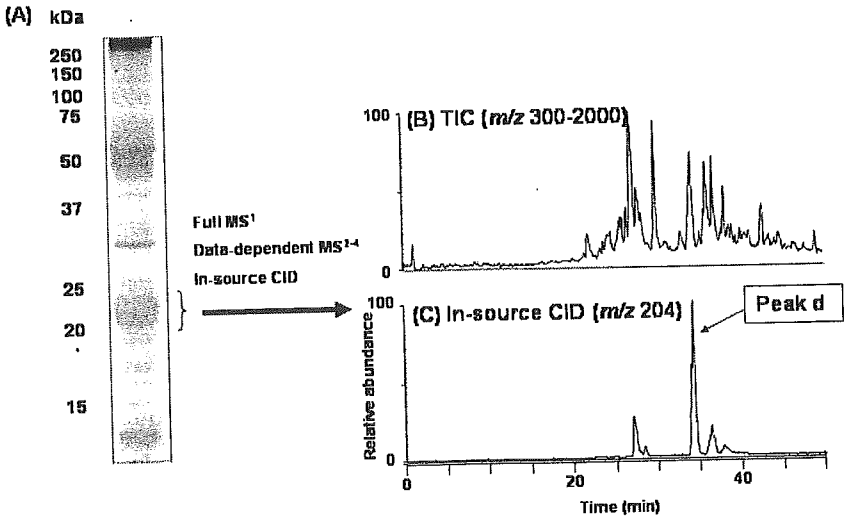

図9　(A) マウス脳由来GPIアンカー型タンパク質のSDS-PAGE、(B) 20-23kDaタンパク質トリプシン消化物のLC/MS、及び(C) インソースフラグメンテーションによって生じた*m/z* 204イオンのマスクロマトグラム

サンプル：20-23kDaに泳動されたタンパク質を1％SDSで抽出しトリプシン消化した
LC/MS：図6に準ずる

ペプチドは MS^2 及び MS^3 により決定した。一例として**図10** に、**図9C** のピークd のデータ依存的 MS^2 及び MS^3 スペクトルを示す。フラグメントパターンからそれぞれ糖鎖配列、及びペプチド配列を図のように推定することができた。同様にすべての糖ペプチドの $MS^{2,3}$ スペクトルを解析することによって、Thy-1 の Asn23, 74, 及び 94 に結合している*N*結合型糖鎖の構造を明らかにすることができた[33]。現在では、クーマシー染色される程度の糖タンパク質から、かなりの糖鎖構造情報を得ることが可能となってきた。

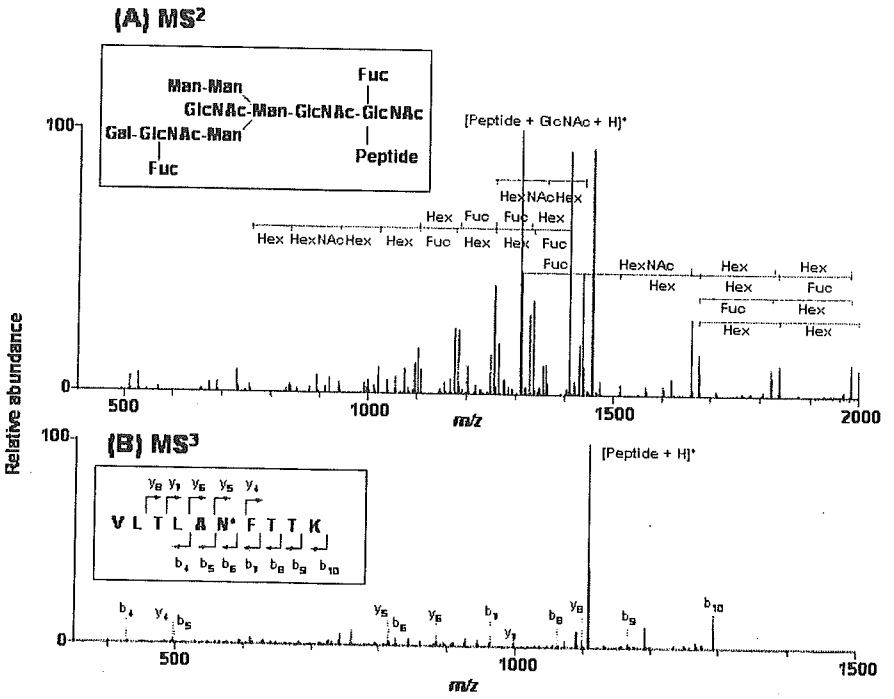

図10　図9中のピークdの(A)データ依存的MS^2スペクトル、及び(B)データ依存的MS^3スペクトル

おわりに

LC/MSとデータベース検索を基盤技術とするプロテオミクスの手法を糖鎖生物学分野に導入することによって、これまで「解析困難」と考えられていた細胞内糖タンパク質の構造特性が、誰にでも簡単に明らかにできるようになってきた。今後、これらのグライコーム解析技術が、診断や治療法の開発を目的とした疾患関連糖鎖・糖タンパク質の研究に貢献できるようになるものと期待される。

謝辞

本稿で紹介した内容は、創薬等ヒューマンサイエンス総合研究事業、日本学術振興会科学研究費補助金、厚生労働科学研究費補助金、並びにCRESTの支援を受けて実施した研究成果をまとめたものである。

■文　献

1) Hermjakob H, Montecchi-Palazzi L, Bader G, Wojcik J, Salwinski L, Ceol A, Moore S, Orchard S, Sarkans U, von Mering C, Roechert B, Poux S, Jung E, Mersch H, Kersey P, Lappe M, Li Y, Zeng R, Rana D, Nikolski M, Husi H, Brun C, Shanker K, Grant SG, Sander C, Bork P, Zhu W, Pandey A, Brazma A, Jacq B, Vidal M, Sherman D, Legrain P, Cesareni G, Xenarios I, Eisenberg D, Steipe B, Hogue C, Apweiler R: The HUPO PSI's molecular interaction format--a community standard for the representation of protein interaction data, Nat Biotechnol, **22**: 177-183, 2004.

2) Schachter H: Congenital disorders involving defective N-glycosylation of proteins, Cell Mol Life Sci, **58**: 1085-1104, 2001.

3) Lowe JB, Stoolman LM, Nair RP, Larsen RD, Berhend TL, Marks RM: ELAM-1--dependent cell adhesion to vascular endothelium determined by a transfected human fucosyltransferase cDNA, Cell, **63**: 475-484, 1990.

4) Phillips ML, Nudelman E, Gaeta FC, Perez M, Singhal AK, Hakomori S, Paulson JC: ELAM-1

mediates cell adhesion by recognition of a carbohydrate ligand, sialyl-Lex, Science, **250**: 1130-1132, 1990.
5) Dennis JW, Granovsky M, Warren CE: Glycoprotein glycosylation and cancer progression, Biochim Biophys Acta, **1473**: 21-34, 1999.
6) Delves PJ: The role of glycosylation in autoimmune disease, Autoimmunity, **27**: 239-253, 1998.
7) Gleeson PA: Glycoconjugates in autoimmunity, Biochim Biophys Acta, **1197**: 237-255, 1994.
8) Chui D, Sellakumar G, Green R, Sutton-Smith M, McQuistan T, Marek K, Morris H, Dell A, Marth J: Genetic remodeling of protein glycosylation in vivo induces autoimmune disease, Proc Natl Acad Sci U S A, **98**: 1142-1147, 2001.
9) 三善英知、谷口直之：プロテオミクスから機能グライコミクスへ：糖鎖の機能解明の重要性、生化学、**76**: 1337-1343, 2004.
10) Taniguchi N, Ekuni A, Ko JH, Miyoshi E, Ikeda Y, Ihara Y, Nishikawa A, Honke K, Takahashi M: A glycomic approach to the identification and characterization of glycoprotein function in cells transfected with glycosyltransferase genes, Proteomics, **1**: 239-247, 2001.
11) Morelle W, Michalski JC: Glycomics and mass spectrometry, Curr Pharm Des, **11**: 2615-2645, 2005.
12) Dell A, Morris HR: Glycoprotein structure determination by mass spectrometry, Science, **291**: 2351-2356, 2001.
13) Kaji H, Saito H, Yamauchi Y, Shinkawa T, Taoka M, Hirabayashi J, Kasai K, Takahashi N, Isobe T: Lectin affinity capture, isotope-coded tagging and mass spectrometry to identify N-linked glycoproteins, Nat Biotechnol, **21**: 667-672, 2003.
14) Qiu R, Regnier FE: Use of multidimensional lectin affinity chromatography in differential glycoproteomics, Anal Chem, **77**: 2802-2809, 2005.
15) Hase S, Ikenaka T, Matsushima Y: A highly sensitive method for analyses of sugar moieties of glycoproteins by fluorescence labeling, J Biochem (Tokyo), **90**: 407-414, 1981.
16) Tomiya N, Awaya J, Kurono M, Endo S, Arata Y, Takahashi N: Analyses of N-linked oligosaccharides using a two-dimensional mapping technique, Anal Biochem, **171**: 73-90, 1988.
17) Takahashi N, Nakagawa H, Fujikawa K, Kawamura Y, Tomiya N: Three-dimensional elution mapping of pyridylaminated N-linked neutral and sialyl oligosaccharides, Anal Biochem, **226**: 139-146, 1995.
18) Suzuki-Sawada J, Umeda Y, Kondo A, Kato I: Analysis of oligosaccharides by on-line high-performance liquid chromatography and ion-spray mass spectrometry, Anal Biochem, **207**: 203-207, 1992.
19) Lattova E, Perreault H: Profiling of N-linked oligosaccharides using phenylhydrazine derivatization and mass spectrometry, J Chromatogr A, **1016**: 71-87, 2003.
20) Kawasaki N, Ohta M, Hyuga S, Hashimoto O, Hayakawa T: Analysis of carbohydrate heterogeneity in a glycoprotein using liquid chromatography/mass spectrometry and liquid chromatography with tandem mass spectrometry, Anal Biochem, **269**: 297-303, 1999.
21) Kawasaki N, Ohta M, Itoh S, Hyuga M, Hyuga S, Hayakawa T: Usefulness of sugar mapping by liquid chromatography/mass spectrometry in comparability assessments of glycoprotein products, Biologicals, **30**: 113-123, 2002.
22) Itoh S, Kawasaki N, Ohta M, Hyuga M, Hyuga S, Hayakawa T: Simultaneous microanalysis of N-linked oligosaccharides in a glycoprotein using microbore graphitized carbon column liquid chromatography-mass spectrometry, J Chromatogr A, **968**: 89-100, 2002.
23) Kawasaki N, Haishima Y, Ohta M, Itoh S, Hyuga M, Hyuga S, Hayakawa T: Structural analysis of sulfated N-linked oligosaccharides in erythropoietin, Glycobiology, **11**: 1043-1049, 2001.
24) Hashii N, Kawasaki N, Itoh S, Hyuga M, Kawanishi T, Hayakawa T: Glycomic/glycoprteomic analysis by liguid chromatography/mass spectrometry : Analysis of glycan structural alteration in cells Proteomics,In press.
25) Takegawa Y, Deguchi K, Ito S, Yoshioka S, Nakagawa H, Nishimura S: Structural assignment of isomeric 2-aminopyridine-derivatized oligosaccharides using negative-ion MSn spectral matching, Rapid Commun Mass Spectrom, **19**: 937-946, 2005.
26) Takegawa Y, Deguchi K, Ito S, Yoshioka S, Sano A, Yoshinari K, Kobayashi K, Nakagawa H, Monde K, Nishimura S: Assignment and quantification of 2-aminopyridine derivatized oligosaccharide isomers coeluted on reversed-phase HPLC/MS by MSn spectral library, Anal Chem, **76**: 7294-7303, 2004.
27) Domon B, Costello CE: Structure elucidation of glycosphingolipids and gangliosides using high-performance tandem mass spectrometry,